

INFORMATION TO USERS

This manuscript has been reproduced from the microfilm master. UMI films the text directly from the original or copy submitted. Thus, some thesis and dissertation copies are in typewriter face, while others may be from any type of computer printer.

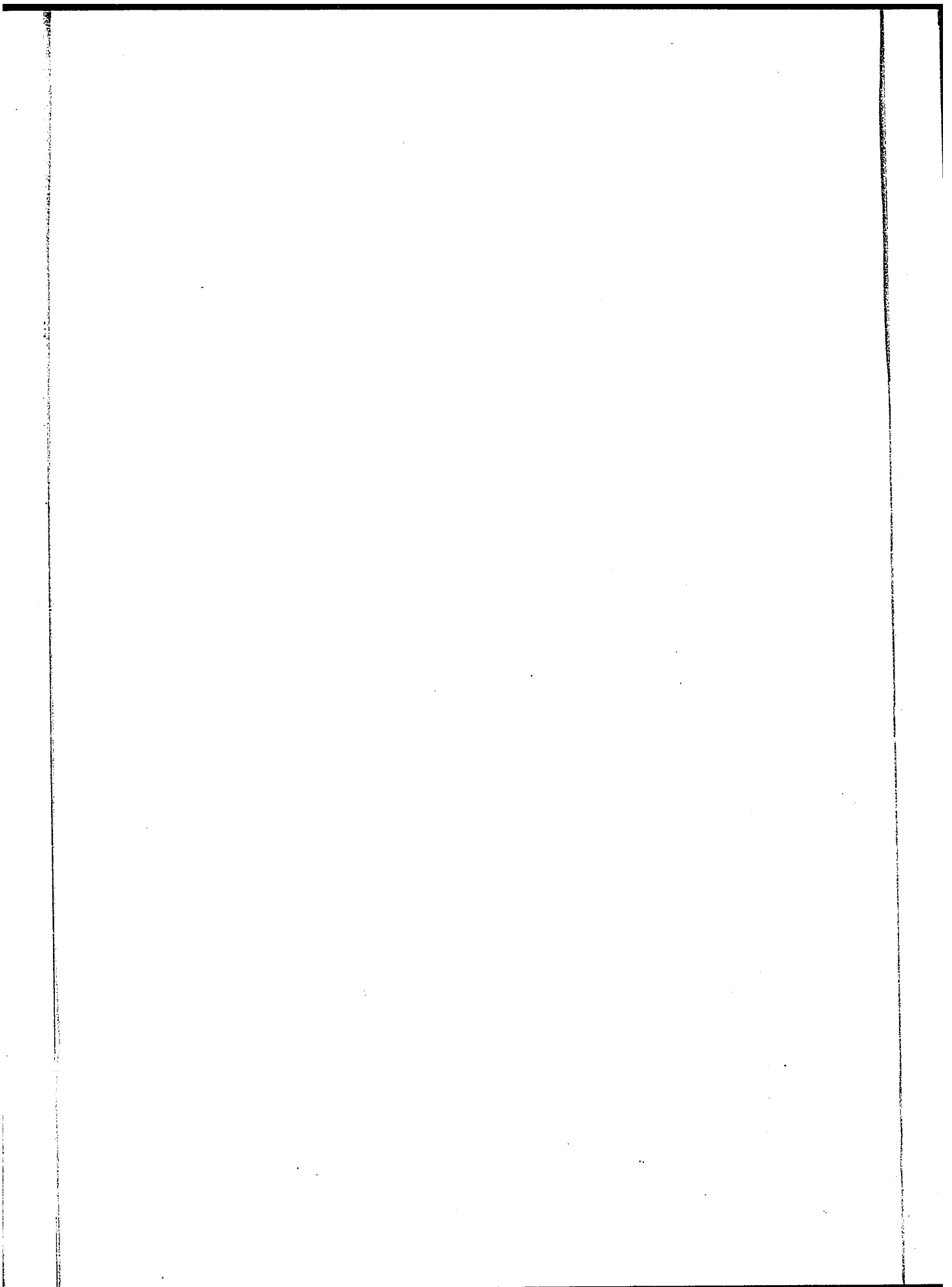
The quality of this reproduction is dependent upon the quality of the copy submitted. Broken or indistinct print, colored or poor quality illustrations and photographs, print bleedthrough, substandard margins, and improper alignment can adversely affect reproduction.

In the unlikely event that the author did not send UMI a complete manuscript and there are missing pages, these will be noted. Also, if unauthorized copyright material had to be removed, a note will indicate the deletion.

Oversize materials (e.g., maps, drawings, charts) are reproduced by sectioning the original, beginning at the upper left-hand corner and continuing from left to right in equal sections with small overlaps.

ProQuest Information and Learning
300 North Zeeb Road, Ann Arbor, MI 48106-1346 USA
800-521-0600

UMI[®]



UNIVERSITY OF OTTAWA

CONSTRUCTION OF A HIGH PRECISION
MICROSCOPE STAGE AND ITS APPLICATION
TO THE
INTERACTION OF 6.2 BEV. PROTONS
WITH EMULSION NUCLEI.

by

John Ancsin



Submitted in partial fulfillment
of the requirements for the degree of
Master of Science.

Department of Physics,
Faculty of Pure and Applied Science,
The University of Ottawa,
Ottawa, Canada.

1960

UMI Number: EC52209

INFORMATION TO USERS

The quality of this reproduction is dependent upon the quality of the copy submitted. Broken or indistinct print, colored or poor quality illustrations and photographs, print bleed-through, substandard margins, and improper alignment can adversely affect reproduction.

In the unlikely event that the author did not send a complete manuscript and there are missing pages, these will be noted. Also, if unauthorized copyright material had to be removed, a note will indicate the deletion.

UMI[®]

UMI Microform EC52209
Copyright 2007 by ProQuest LLC
All rights reserved. This microform edition is protected against
unauthorized copying under Title 17, United States Code.

ProQuest LLC
789 East Eisenhower Parkway
P.O. Box 1346
Ann Arbor, MI 48106-1346

Approved for the
Department of Physics

Supervisor

Chairman of the Examining Committee

Chairman of the Department

ABSTRACT

In the first part of this work the construction of a high precision microscope stage is described with particular reference to a compensating system using two pulleys. The noise measurement of this stage is made by means of an electronic system which measures noise down to a few Angstrom units.

The second part is a study of the stars produced by the interaction of 6.2 Bev. protons with emulsion nuclei. The angular distribution of the pions is found in the laboratory system after reconsidering the definition of the shower particles. The results obtained indicate that in the collision of 6.2 Bev. protons with complex nuclei 3 or 4 nucleons of the target nucleus are directly involved in the pion production. The charged pion multiplicity is found to be $2.5 \pm .2$ per star. These results are in agreement with those predicted by the tunnel theories.

ACKNOWLEDGEMENT

I wish to express my deep sense of gratitude to Mr. J. Hébert for suggesting the problems, for his able guidance and constant encouragement during the progress of this work.

I am greatly indebted to the Reverend Oblates of the University of Ottawa for awarding me a Rector's Bursary and to Professor J. M. Robson for obtaining financial help to enable me to complete my studies.

Acknowledgement is extended to Dr. J. Jarvis, Mr. J. Lefaiivre, Dr. R. C. Smith and my student colleagues for their interest in this work, and for many helpful discussions.

I am also grateful to Mr. C. N. Goodchild for his very valuable help in constructing the microscope stage, and to Miss R. M. Ralph for accepting the typing of the thesis.

LIST OF FIGURES

<u>Number</u>	<u>Page</u>
1. Normalized grain density vs. $p\beta$ for protons, k-particles and pions - - - - -	5
2. The coordinate method of multiple scattering measurement - - - - -	5
3-9. Principle of operation of the scattering microscope stage - - - - -	10
10. Diagram of pulley - - - - -	-14
11. Block diagram of the noise measuring apparatus - - - - -	-21
12. Noise controlled oscillator - - - - -	-21
13. Crystal controlled oscillator - - - - -	-21
14. Mixer - - - - -	-21
15. Stage noise vs. cell length - - - - -	-26
16. Kinetic energy available in C.M. system as a function of the number of target nucleus masses - - - - -	30
17. Curves representing the transformation of angles between the laboratory system and different C.M. systems - - - - -	37
18. Graph showing the dependence of the shower multiplicity on the number of evaporation secondaries - - - - -	-44
19. Energy distribution of the shower particles in the laboratory system - - - - -	44
20. Differential distribution of pions vs. $\log(\tan \theta_L)$, and the best fit gaussian curve - - - - -	-52
21. The dependence of $\log \gamma_c$ on the number of effective nucleon masses - - - - -	-52
22-27. Distribution of pions in different C.M. systems - - - - -	55

CONTENT

	<u>PAGE</u>
ABSTRACT -	i
ACKNOWLEDGEMENT	ii
LIST OF FIGURES	iii

PART I.

MICROSCOPE STAGE AND NOISE MEASUREMENT.

Introduction -	1
Identification and energy determination of charged particles -	2
The problem of the scattering stage and of the noise -	7
Principle of operation -	9
Measurement of noise -	-16
Interferometric method -	-16
Parallel plate condenser method -	17
1) Principle of Kerr cell -	17
2) Noise measurement by measuring frequency -	18
Description of the complete system -	22

PART II.

PAGE

INTERACTION OF 6.2 BEV. PROTONS
WITH THE EMULSION NUCLEI.

Multiplicity - - - - -	28
Tunnel theory - - - - -	29
Angular distribution - - - - -	32
Transformation of angles - - - - -	32

EXPERIMENTAL PART.

Procedure - - - - -	40
Shower multiplicities - - - - -	41
Pion multiplicity - - - - -	43
Angular distribution - - - - -	50
1) From the determination of the half angle - - - - -	50
2) From the determination of γ_c - -	50
3) From the distribution plotted in different C.M. systems - - - -	53
Conclusion - - - - -	56
Appendix - - - - -	58

PART I.

MICROSCOPE STAGE AND NOISE MEASUREMENT.

INTRODUCTION.

It is a well known experimental fact that charged particles ionize the matter through which they travel. Making use of this fact, the photo emulsion technique has been developed as an important tool for investigating the interaction of elementary particles.

Our main purpose will be the analysis of the events resulting from the interaction of 6.2 Bev. protons with the nuclei of the emulsion.

To study an event, one has to know the identity and the energy of the primary, the target and the particles produced, if any, in the interaction. Every analysis, therefore, has to start with the identification and energy determination of the particles involved. Unfortunately, the neutral particles are not registered in the plates, and distinction between positive and negative charges is not possible in the absence of a magnetic field.

Due to the fact that all of this work is based on the identification of the elementary particles, it would be worthwhile to say a few words about the way of doing this, and point out the problems to be overcome. First the basic principles of identification and energy determination will be summarized, the formulae used stated and the importance of the

good scattering microscope stage explained. Finally the problem of multiplicity and angular distribution of pions (π -mesons) produced in the above mentioned interaction will be discussed.

IDENTIFICATION AND ENERGY DETERMINATION OF CHARGED PARTICLES.

A charged particle traversing matter will lose energy due to the interaction with the atoms of the matter. In the photo emulsion this interaction consists of the ionization of the individual atoms and appears in the form of grains when looking at it through a microscope. Knowing that the ionization is the interaction of the incoming primary particle with the periphery electrons of the target atoms and that this interaction is governed by Coulomb's law, it can be shown that the energy loss of the primary per unit length (commonly called the ionization) is given by the following relation:

$$(1) \quad \frac{dE}{dx} = k \frac{m^2 Z^2}{p^2} \ln c E$$

where p , m and Z are the momentum, the mass and the charge of the primary, respectively, and k and c are constants.

For the derivation of this formula it has been assumed that the electrons revolving around the atom are so slow in comparison with the primary that it can be assumed that they

are at rest. This assumption means that equation (1) can be applied only if the particle under consideration is fast enough for its energy to be higher than a certain limit E_0 . Below this energy equation (1) has no meaning.

It is clear from this formula that below the relativistic region the ionization at a given momentum and charge is proportional to the square of the mass. This fact is used to determine the mass of a particle simply by measuring its momentum and the so-called grain density, using figure 1 which is equation (1) plotted for protons, pions and K-particles, the rest mass energies being 937 Mev., 140 Mev., and about 480 Mev., respectively. The grain density is the number of grains per unit length, i.e. the ionization. These are particles of unit charge. On the other hand the grain density at a given mass and momentum is proportional to the square of the charge. Thus, particles with $Z = 2$ would have four times as high a grain density as a particle having the same mass and momentum, but unit charge. Notice also that the curves in figure 1 have a minimum and in the high energy region a mass and energy independent portion called the plateau.

Let us turn now to the problem of energy determination. Energy measurement is most commonly done by multiple scattering measurements.

When a particle with high enough velocity travels in matter it will, in general, in addition to the ionization, suffer elastic collision with the nuclei of the atoms. This being again an electrostatic interaction will be described by Coulomb's law, and consequently the relation between the angle of scattering and the energy of the primary will be given by Rutherford's scattering equation. For multiple scattering of the primary, using Rutherford's relation for small angles, it can be shown that

$$(2) \quad p\beta = \frac{k}{\alpha}$$

where p is the momentum of the primary, $\beta = \frac{v}{c}$, K is a constant given by equation (3) and $\bar{\alpha}$ is the mean angle of multiple scattering.

$$(3) \quad K = f(t)$$

Here t is the cell length used in microns (explained further on). For the derivation of equations (1) and (2) see reference (1) and for equation (3) see (2). Equation (2) is used in practice for momentum determination in the range of about 20 Mev. $< E < 10$ Bev. One can have the impression when looking at equation (2) that it is necessary to measure each

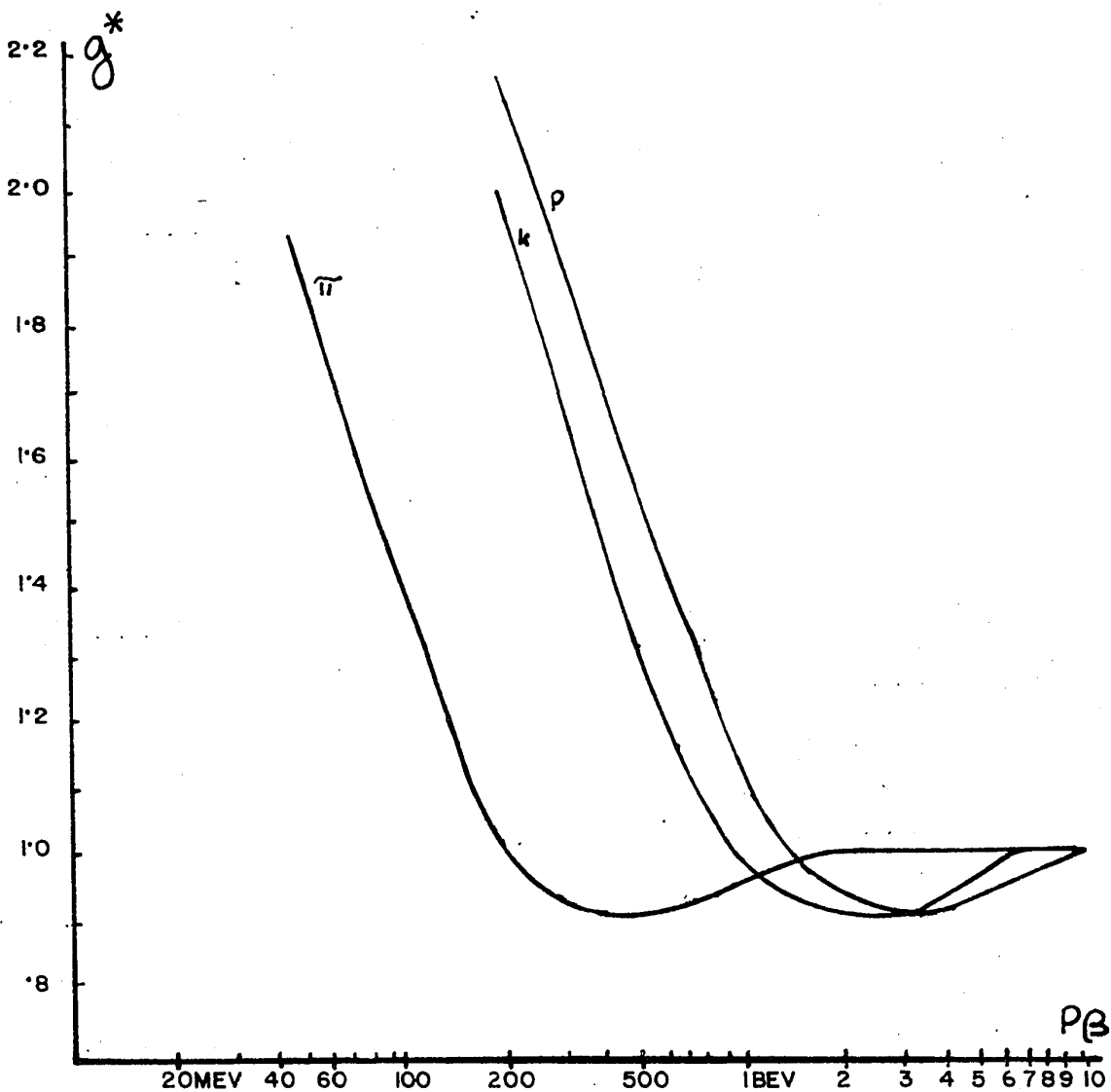


FIG.1 NORMALISED GRAIN DENSITY VS. $p\beta$, FOR PIONS , K-PARTICLES AND PROTONS .

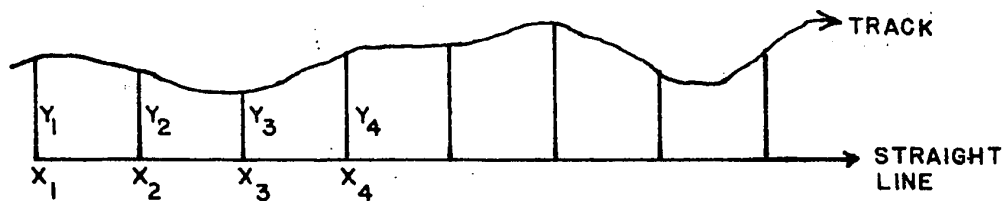


FIG.2. THE COORDINATE METHOD OF MULTIPLE SCATTERING MEASUREMENT

scattering angle of a given particle in order to determine its energy. To avoid this misconception it is necessary to describe briefly the technique of angle measurement.

There are a number of different ways of determining the scattering angles. For a short summary of them see (3). In our measurement we used the so-called coordinate method of Fowler, which can be described as follows:

Consider a particle moving in matter suffering multiple collisions as shown in figure 2. For small angles the tangent of an angle is equal to the angle itself. Therefore, instead of measuring the actual angles it is sufficient to measure the tangents. Moreover, if for measuring the tangents we use triangles whose two shorter sides are along the x and y axes, and if the side along the x direction has unit length, then it is sufficient to measure only the y component of the triangle for determining the tangent of the scattering angle. Let the particle whose scattering angle is to be determined be displaced along a perfectly straight line; then let us measure its perpendicular displacement with respect to this straight line, at each unit length as shown in figure 2. From these readings, $y_1, y_2, y_3, \dots, y_n$, the angles can be determined in the following way: The first differences $(y_n - y_{n-1})$ give the curvature of the track, and the second ones

$(y_n - y_{n-1}) - (y_{n-1} - y_{n-2})$ will give the angles of scattering. Finally we obtain the mean angle $\bar{\alpha}$, necessary to calculate the momentum of the particle. Knowing the momentum and the mass, the energy can be calculated.

THE PROBLEM OF THE SCATTERING STAGE AND OF THE NOISE.

There is one very important thing assumed in the above described angle measurement. We assumed that it is possible to displace the path of a particle along a perfectly straight line. It is quite easy to show, however, that it cannot be done. To show this let us consider the way of displacing the path of a particle in practice.

When measuring the angles using the method described, the photo emulsion plate is placed on the stage of a microscope. The track of the particle is lined up parallel to the direction along which the stage is displaced with the aid of the microscope fixed to the base of the microscope. The scattering angles along the path of the particle are then measured as described above by means of an eyepiece fixed to the microscope head. Now, the assumption in question is that the microscope stage is capable of doing displacement along a perfectly straight line. This, of course, is an assumption that can be accepted when measuring relatively low energies where the scattering

angles are relatively large. At high energies, however, this assumption can seriously be questioned for the following reason:

Most of the previously used microscope stages have a rigid part fixed to the base of the microscope with their top as smoothly finished as possible. An equally well finished movable part is placed on top of this with a thin film of oil between them to provide a smooth straight motion of the latter when pushed with a micrometer. Obviously the surfaces obtained this way will not be as flat as to provide motion in a geometrically flat plane but rather a zig-zag motion about this plane. This small irregularity is called the noise.

To have an idea about the order of magnitude of this noise one can express it in terms of energy. If we would have a geometrically straight line placed on top of the stage, then doing scattering measurements on it we should find no scattering at all if the stage were perfect. In practice, however, we would find for a well built mechanical stage that this energy is of the order of 2 to 3 Bev. This means that the stage due to its noise cannot measure energies higher than, say, 1.5 to 2 Bev. This simple illustration shows the importance of having as good stages as possible, especially if one deals with events

where the energies involved are higher than 2 or 3 Bev. In our case the primary protons have 6.2 Bev. kinetic energy so that we are justified in considering the problem of noise in detail. It became possible recently to buy better stages on the market, but they are very expensive. Considering the necessity of having a high precision stage, we decided to build one. The principle of operation has been suggested by Plainevaux, see reference (4), and the essence of it is that it has no sliding surfaces, thus avoiding the mechanical noise due to the imperfection of the surfaces.

PRINCIPLE OF OPERATION.

The principle of operation can be explained very easily by making use of the diagrams in figures 3 to 9. Consider the system composed of two identical elastic blades "a". One end of each of them is fixed to the ends of a rigid weightless rod "b", the other end to the rigid frame "A", as shown in figure 3. The length of "b" is chosen so as to make the blades parallel.

After applying the force F along "b" the new position of the system will be that shown in figure 4. Notice that "b" remained parallel to the horizontal.

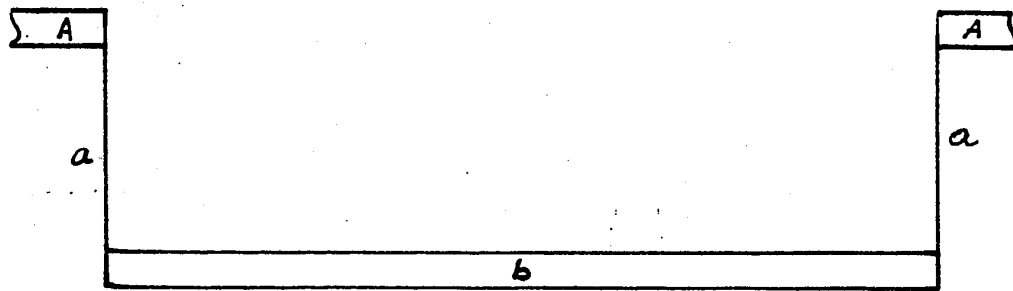


FIG. 3

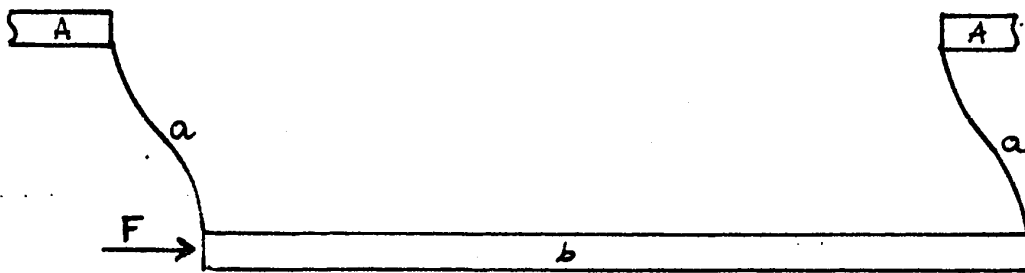


FIG. 4

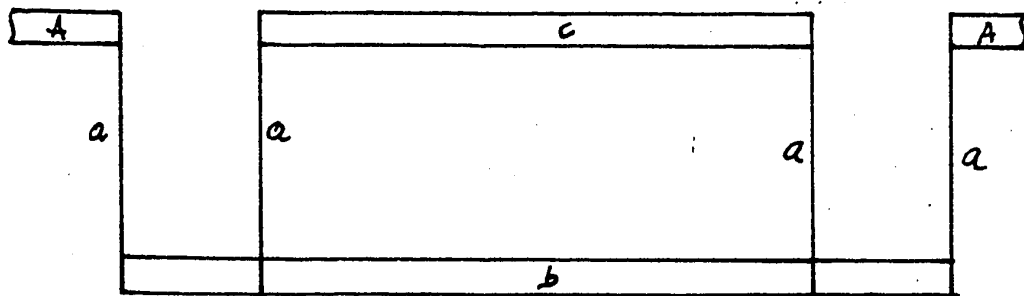


FIG. 5

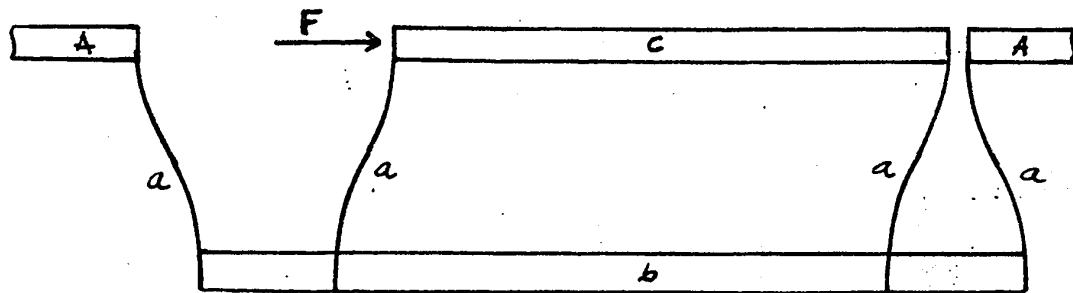
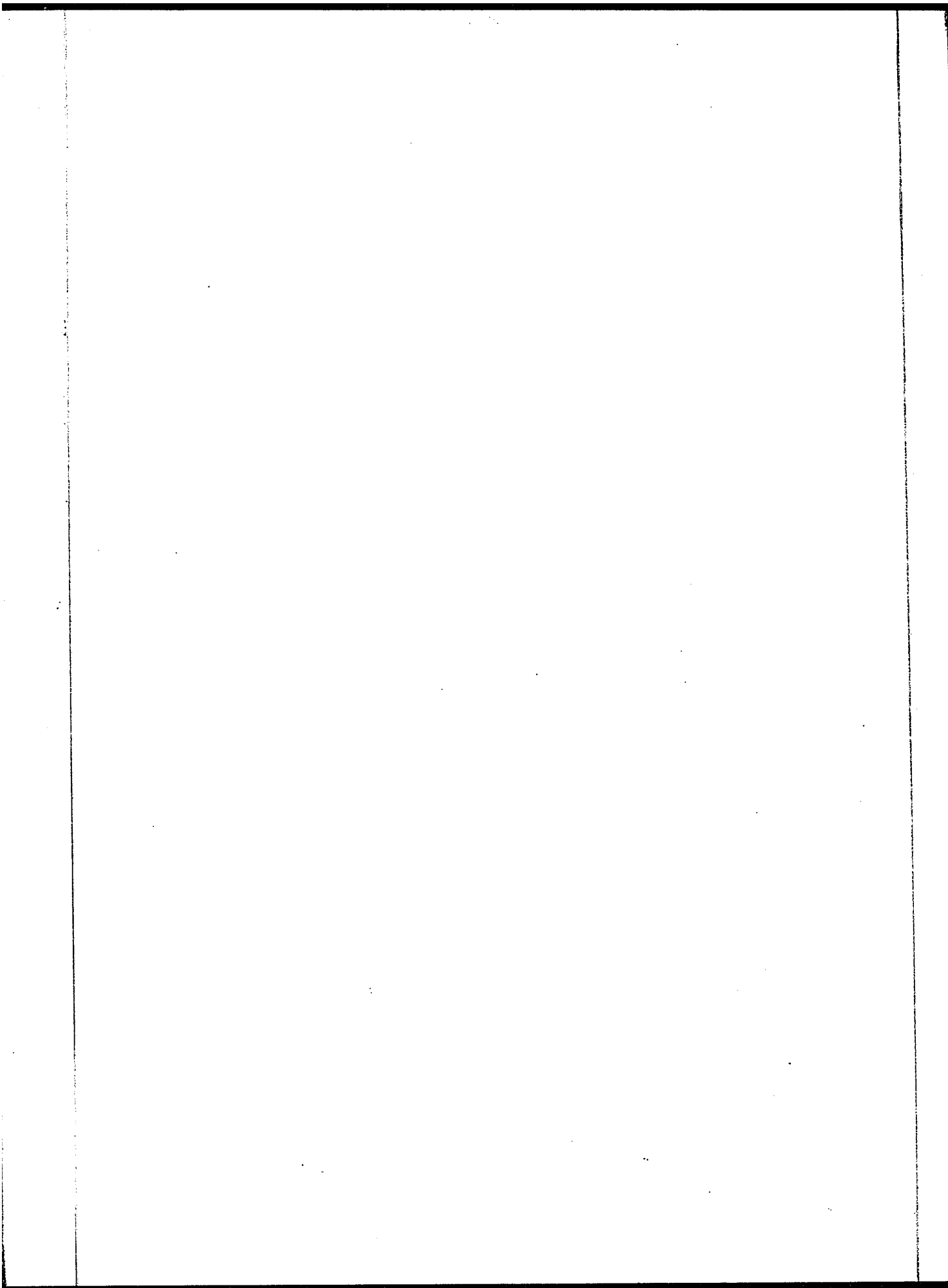


FIG. 6



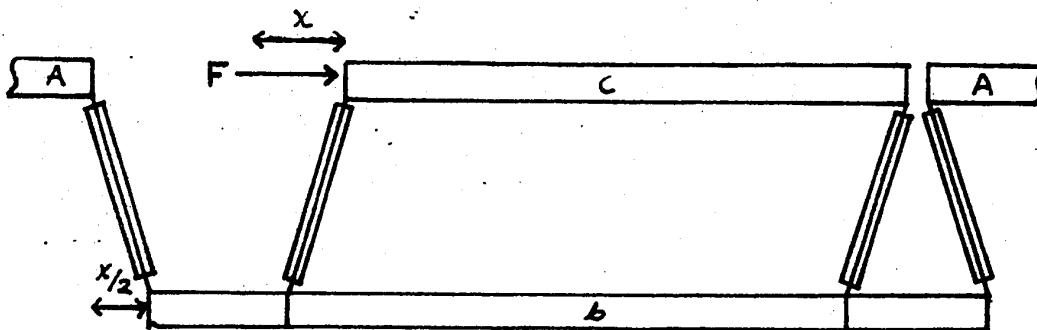


FIG. 7

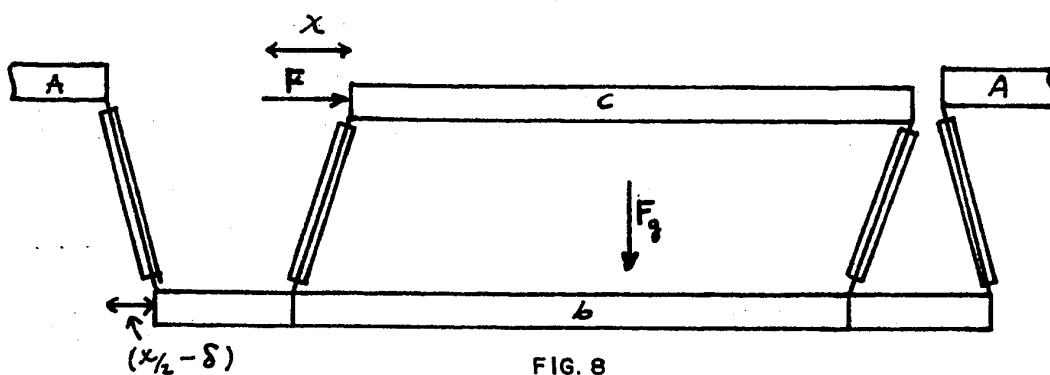


FIG. 8

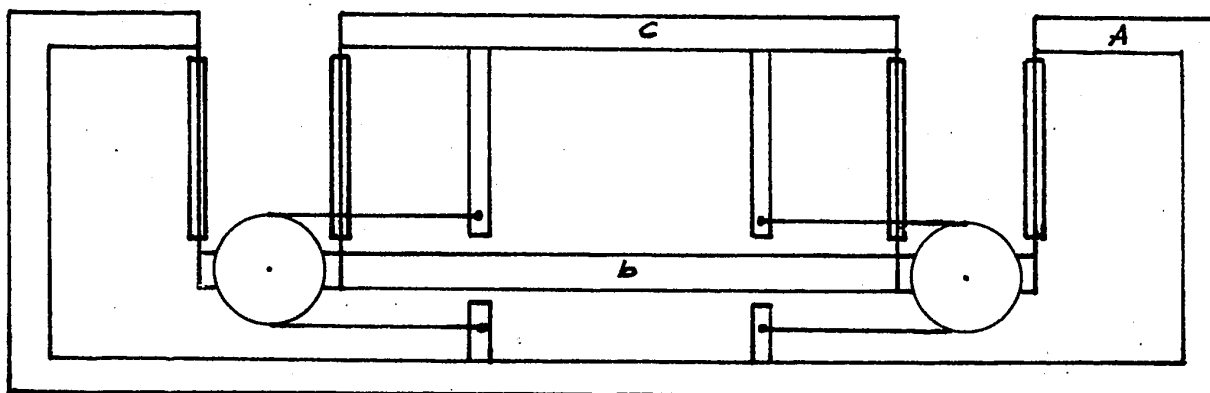
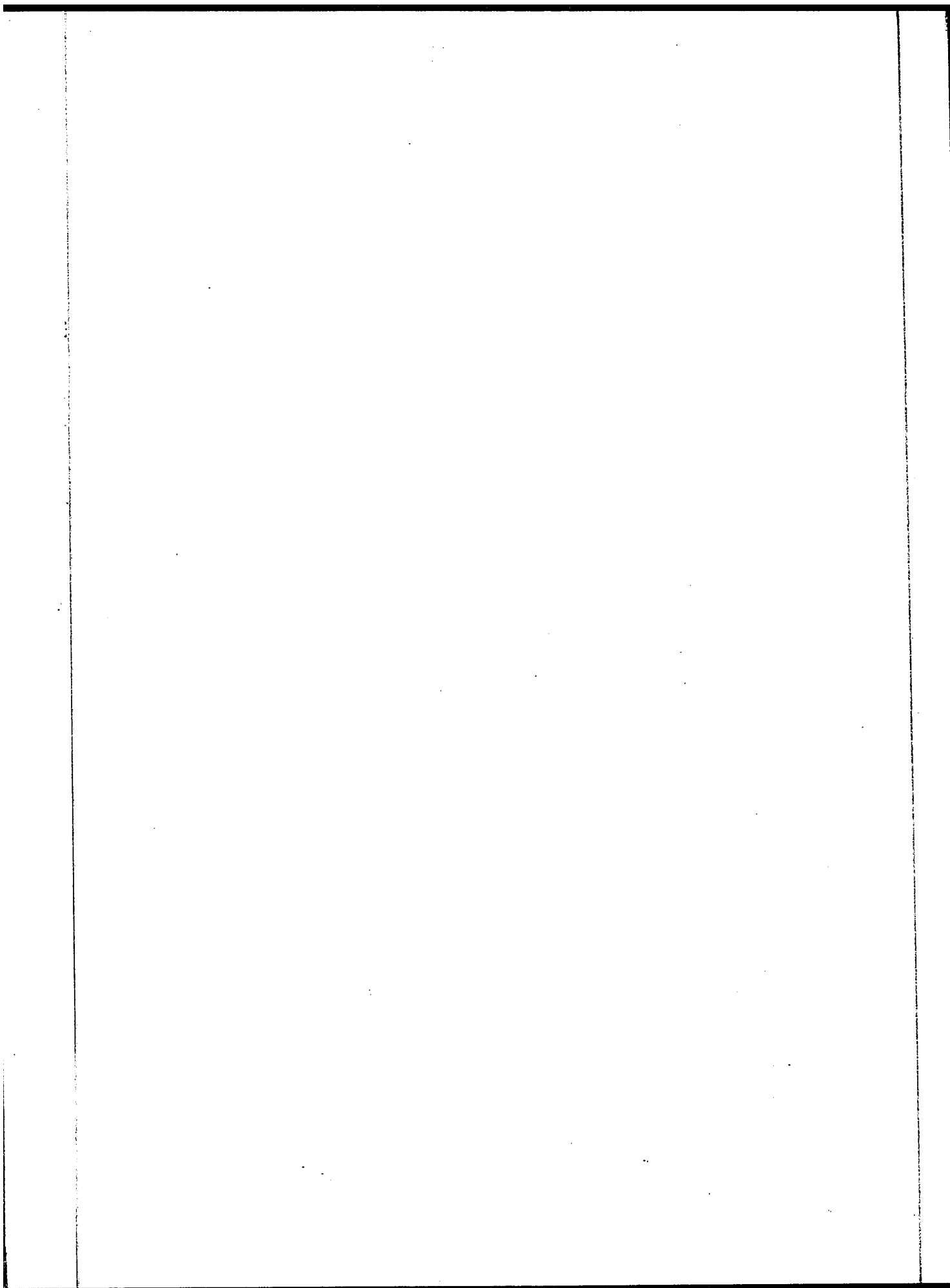


FIG. 9

PRINCIPLE OF OPERATION OF THE
SCATTERING MICROSCOPE STAGE



Let us modify the system to that shown in figure 5. There again all blades are assumed to be identical and parallel in this position. "c" is a weightless rigid rod.

Applying the force F this time along "c", the system will be displaced to a new position, as shown in figure 6.

It will be shown later that it is necessary to make the following modification on the system: let us clamp the blades by two rigid plates in such a way that only a very short part of them will be free to bend. With clamped blades, the system of figure 6 is redrawn in figure 7.

There are three important points to be noticed in connection with figure 7.

(1) Due to the weightlessness of the stage the only external force is F .

(2) Because F acts along the horizontal line, "c" will move in the horizontal plane.

(3) If "c" moves a distance x , "b" moves a distance $x/2$. The stage, however, is not weightless. Let the mass of the stage be m , then at its centre of gravity there is a force F_g , perpendicular to F . As a result of this additional force, the displacement of "c" will not take place along the horizontal.

Let us reconsider the previous three points.

- (1) There are two external forces.
- (2) The resultant does not lie in the horizontal plane, consequently "c" will not move in the horizontal plane.
- (3) If "c" moves a distance x , "b" will not move $x/2$, but less, as shown in figure 8.

It is clear that F_g causes two things:

- (1) Non-horizontal motion of "c" (lowering).
- (2) "b" does not move $x/2$ for a displacement x of "c".

There are two ways of forcing this system back to rectilinear motion. One way would be as follows: The non-linearity of the motion was caused by F_g . Therefore, if we would apply an equal but opposite force $-F_g$ at the centre of gravity of the system the stage would appear weightless again. Alternatively, the linear motion of "c" implies that for a displacement x of "c" there is a displacement $x/2$ of "b". On the other hand, non-linear displacement of "c" causes a displacement of "b" less than $x/2$. Consequently, forcing "b" to be displaced by $x/2$ then "b" would automatically bring "c" back to the horizontal plane, i.e. its motion will be rectilinear again. For practical purposes the first way would not be satisfactory because the application of $-F_g$ would make the stage rather awkward looking, and in addition the adjustment of the

position and magnitude of the force $-F_g$ could be difficult. For this practical reason only, we discard this possibility and examine the other.

A solution of the problem was given by Plainevaux. In his stage he applied two micrometers. One pushes "c", the other pushes "b". With the aid of a third screw, through a connecting system, the micrometers are driven in a 1:2 ratio. Stages built this way are known as high energy scattering stages, and are commercially available. There are some disadvantages, however, in this arrangement.

Due to backlash in the micrometer screws they will never start to move exactly in a 1:2 ratio. This will become even worse due to wear. Another thing is that these micrometers are more expensive than the ordinary ones because they have to perform two things at the same time. They must be just as accurate as any other type of micrometer and they must be able to push hard without losing their accuracy. None of the commonly used micrometers are designed to perform these two functions. At least two of these screws are necessary in Plainevaux's microscope.

Our solution of the problem is this:

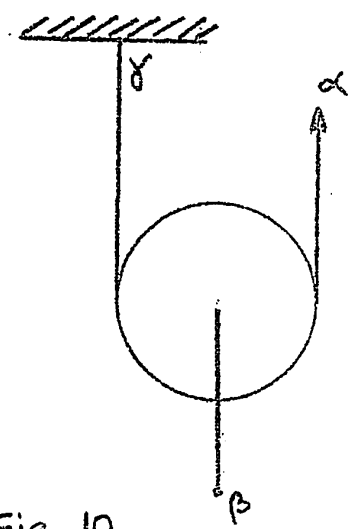


Fig. 10

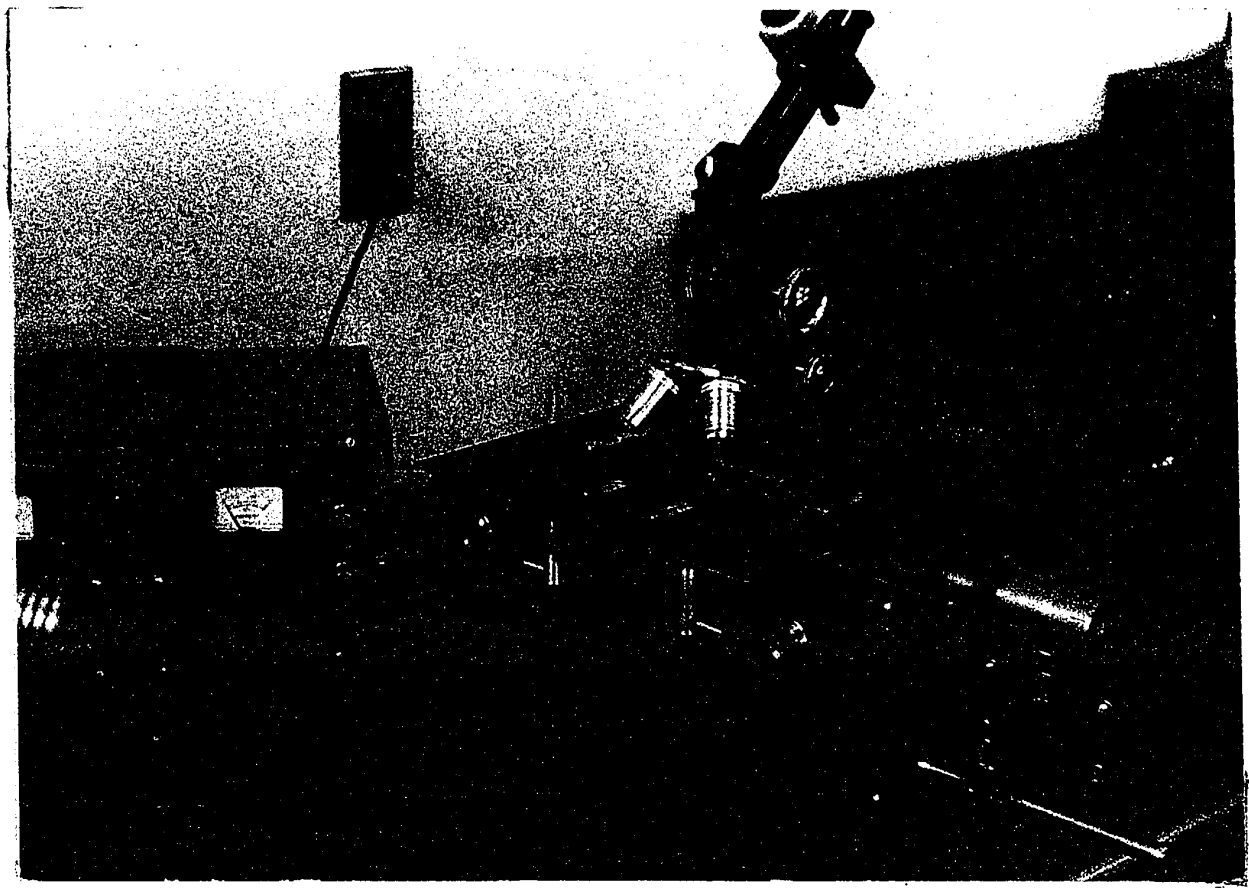
A simple device which divides distances by 2 is a movable pulley. When point "a" moves a distance x , point "β" moves a distance of $x/2$, and the problem is solved. Thus, point "a" should be connected to "c", point "γ" to the rigid frame "A" and the axle of the pulley to part "b"

of figure 8. The advantages of this arrangement over that of Plainevaux are: Because the pulley is driven by "c" and not directly by the micrometer, "b" will be forced to move $x/2$ for a displacement x of "c". Thus the control of "b" would be independent of backlash of the micrometer. Moreover we need only one micrometer instead of two, thus making the stage less expensive. Another point is that making the strings across the pulley tight enough eliminates the backlash in the pulley itself.

It is clear now why it is necessary to clamp the blades. Due to the presence of F_g even the pulley would not bring "c" back to the horizontal because of the elasticity of the blades.

Finally the completed diagram of the system performing the rectilinear motion is given in figure 9.

The photograph of the microscope having the described stage is shown here.



MEASUREMENT OF THE NOISE

To check the reliability of the stage, we have to measure its noise. The measurement of the noise is essentially the problem of measuring small distance changes. The conventional way of doing this is to use interferometry. It seems logical to consider the method of measuring small distances interferometrically as it is done in practice, and show its accuracy; then discuss the possibility of improvements and finally give our solution of the problem.

Interferometric Method.

An interferometer consists of two optically flat semi-transparent surfaces set up parallel to one another. Due to the multiple reflection of light between the plates, an interference pattern can be observed. Knowing the wavelength of the light used and counting the number of fringes, the distance between the surfaces can be calculated. On changing the separation of the plates, one can observe a fringe shift.

To apply this method to noise measurement, one needs to fix one plate of the interferometer to the rigid part of the stage, the other plate to the movable part. We then measure the fringe shift as a function of the displacement of the

movable part of the stage.

Accuracy:

Estimating, for instance, to $1/25$ th of a fringe which corresponds to a distance of $\lambda/50$, and using $\lambda = 5000 \text{ \AA}$, we can determine distances of the order of 100 \AA . Obviously the error can be quite large in this case. One also realizes that the wavelength used sets a lower limit to the magnitude of the distance differences which can be determined in this way. Thus, the limited accuracy made it obvious that it would be worthwhile to look for another principle which, if applied to noise determination, would give better accuracy.

Parallel plate condenser method.

To find a better method, one has to go back to elementary experimental physics and search for principles or known facts by which distances are related sensitively to other quantities. We have chosen two experimental facts which we thought deserved consideration:

(1) The principle of the Kerr cell. It is well known that liquids change their optical properties when passing through an electric field. Let us produce an electric field by a fixed potential difference across a parallel plate condenser. This

field will then be a function of the distance between the plates. Setting these up the same way as the plates of the interferometer, the electric field will then be controlled by the noise of the stage. Passing plane polarized light through the field, the intensity of the light as picked up by a photocell through a fixed Nicol prism will be a function of the stage noise. This way noise can be measured by measuring light intensity. This method looks promising, but the necessity of darkness and the use of liquid would probably make the procedure rather unpleasant. For this reason we decided to look for some other way.

(2) Noise measurement by measuring frequency. A simple way of measuring small distance variations was suggested by Waddington, see reference (5). This method is: Consider a parallel plate condenser, its capacity in e.s.u. is given by

$$C = \frac{A}{4\pi x}$$

where A: area of the surfaces;
 x: distance between the plates.

Using this condenser as a component of a parallel LC circuit, an oscillator can be built whose frequency will be a function of the distance between the plates. One realizes at once that this method can easily be adopted to the noise measurement by setting up the plates of the condenser in the same way as the

plates of the interferometer. Then the stage noise would mean variation in the distance between the plates, and consequently as a result of the noise, we would have a varying capacitance.

From the fundamental relation

$$(4) \quad \omega = \frac{1}{\sqrt{LC}} = \sqrt{\frac{4\pi x}{LA}}$$

we get

$$(5) \quad \frac{\Delta\omega}{\Delta x} = \frac{1}{2} \frac{\omega}{x}$$

Hence, the relation between the noise and the frequency variation of the oscillator is given by

$$(6) \quad \Delta x = 2 \frac{x}{f} \Delta f \quad \text{where } \omega = 2\pi f$$

As an example let us calculate the sensitivity of the oscillator having the following values:

$$\begin{aligned} f &= 1 \text{ Mc/s;} \\ x &= 10^{-2} \text{ cm;} \\ \Delta f &= 1 \text{ c/s;} \end{aligned} \quad \begin{aligned} \text{then } \Delta x &= 2x \frac{10^{-2}}{10^6} \\ &= 2 \times 10^{-8} \text{ cm} \end{aligned}$$

This means that having an oscillator whose frequency is 1 Mc/s with a plate separation of 0.1 mm, a variation of $2 \overset{\circ}{\text{A}}$ would

produce 1 c/s frequency change of the oscillator frequency.

This illustration shows that it is possible to have a much more accurate way of making distance measurements than by interferometry.

Let us consider now what setup is required to perform the noise measurement successfully.

Looking at equation (6), we see that to detect the smallest possible distances we need an oscillator with as high a frequency as possible. On the other hand, the separation of the plates has to be as small as possible.

There are two problems to solve at this point:

- (1) Frequency measurement: We have to determine very small changes in the frequency of the oscillator. It would be impossible to do this directly. However, using a fixed frequency oscillator and a mixer, the difference frequency can be quite small so that relatively small frequency changes can easily be measured.
- (2) Frequency stability of the oscillator: Because the frequency changes due to the noise are to be very small, the frequency stability of the oscillator has to be very good. Fortunately this is again a standard problem and it is well known how the best possible stability can be achieved. The main causes of the frequency shift of an oscillator are the following:

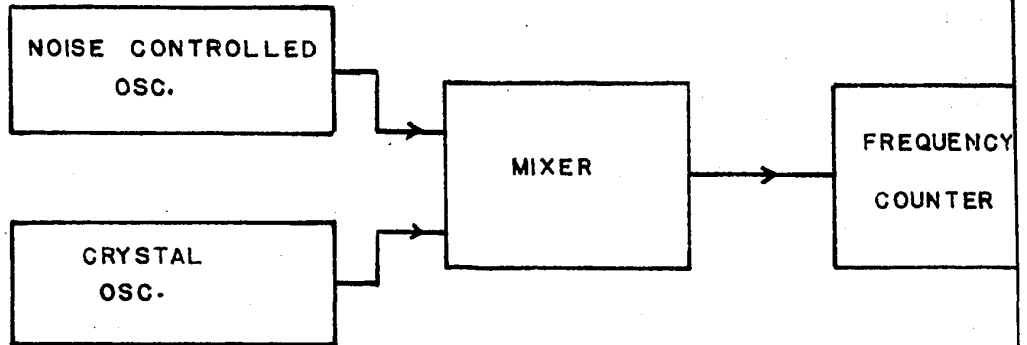


FIG. 11 BLOCK DIAGRAM OF THE NOISE MEASURING APPARATUS.

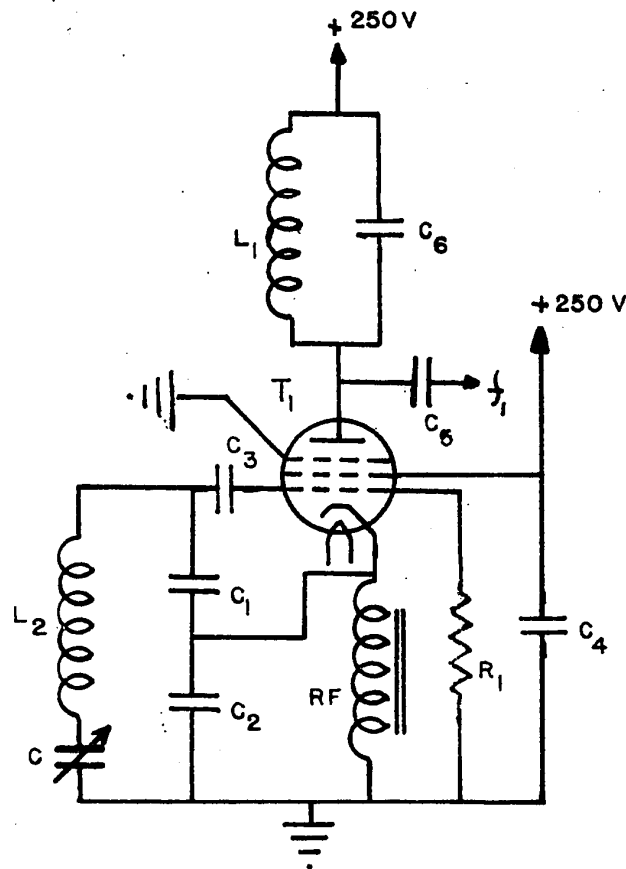


FIG. 12 NOISE CONTROLLED OSCILLATOR

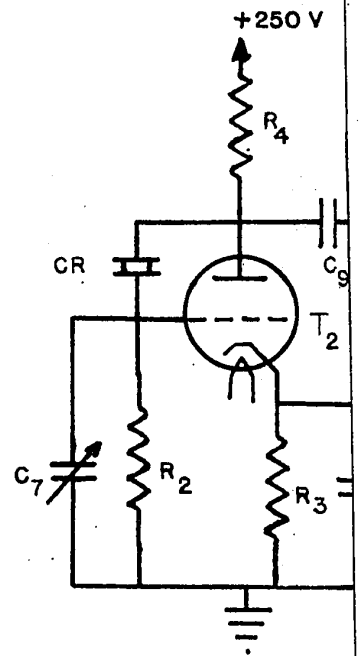
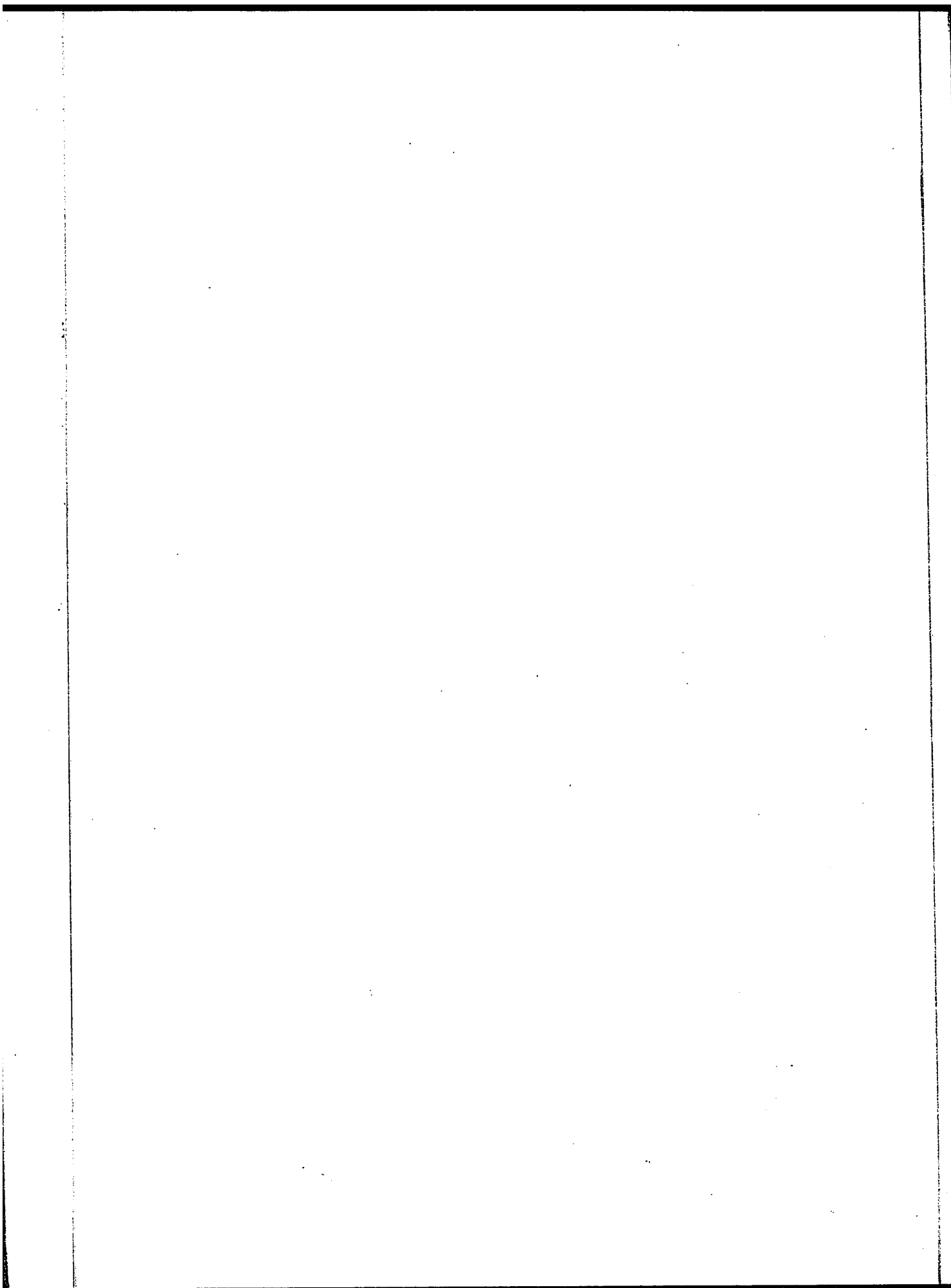


FIG. 13 CRYSTAL CONTROLLED OSCILLATOR



QUENCY
ENTER

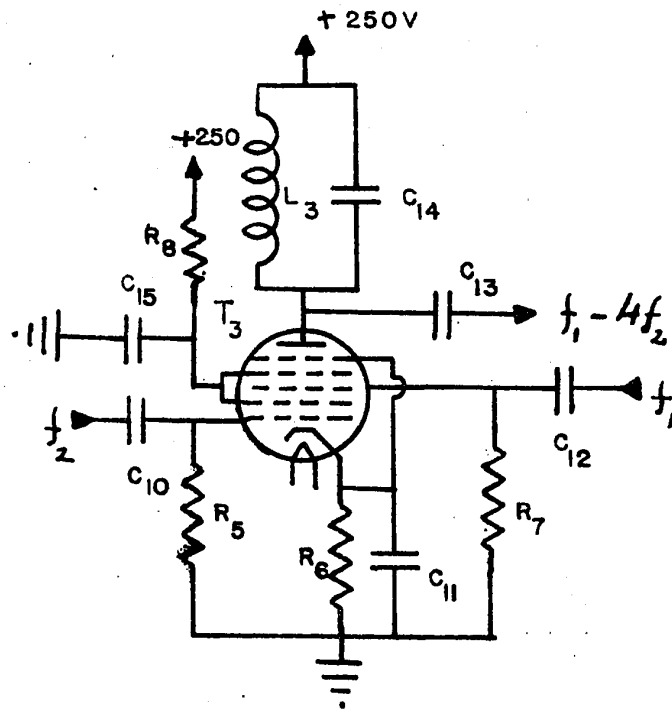
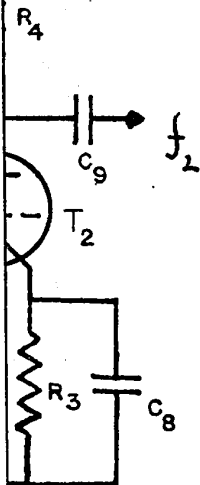


FIG. 14 MIXER

250 V



AL CONTROLLED
ATOR

$$C_1^* = C_2^* = 1000 \mu\mu$$

$$C_3^* = 100 \mu\mu$$

$$C_4 = C_5 = C_{10} = C_{12} = C_{13} = 1000 \mu\mu$$

$$C_6 = 400 \mu\mu$$

$$C_7 = 30-50 \mu\mu$$

$$C_8 = 500 \mu\mu$$

$$C_9 = 100 \mu\mu$$

$$C_{11} = 250 \mu$$

$$C_{14} = .01 \mu$$

$$C_{15} = 10 \mu$$

$$R_1 = 47 K$$

$$R_2 = 270 K$$

$$R_3 = 270 \Omega$$

$$R_4 = 100 K$$

$$R_5 = 22 K$$

$$R_6 = 1 K$$

$$R_7 = R_8 = 68 K$$

$$RF = 2.5 \mu H, 50 \text{ mA RF CHOKE}$$

$$L_1 = 22 \mu H$$

$$L_2 = 62 \mu H$$

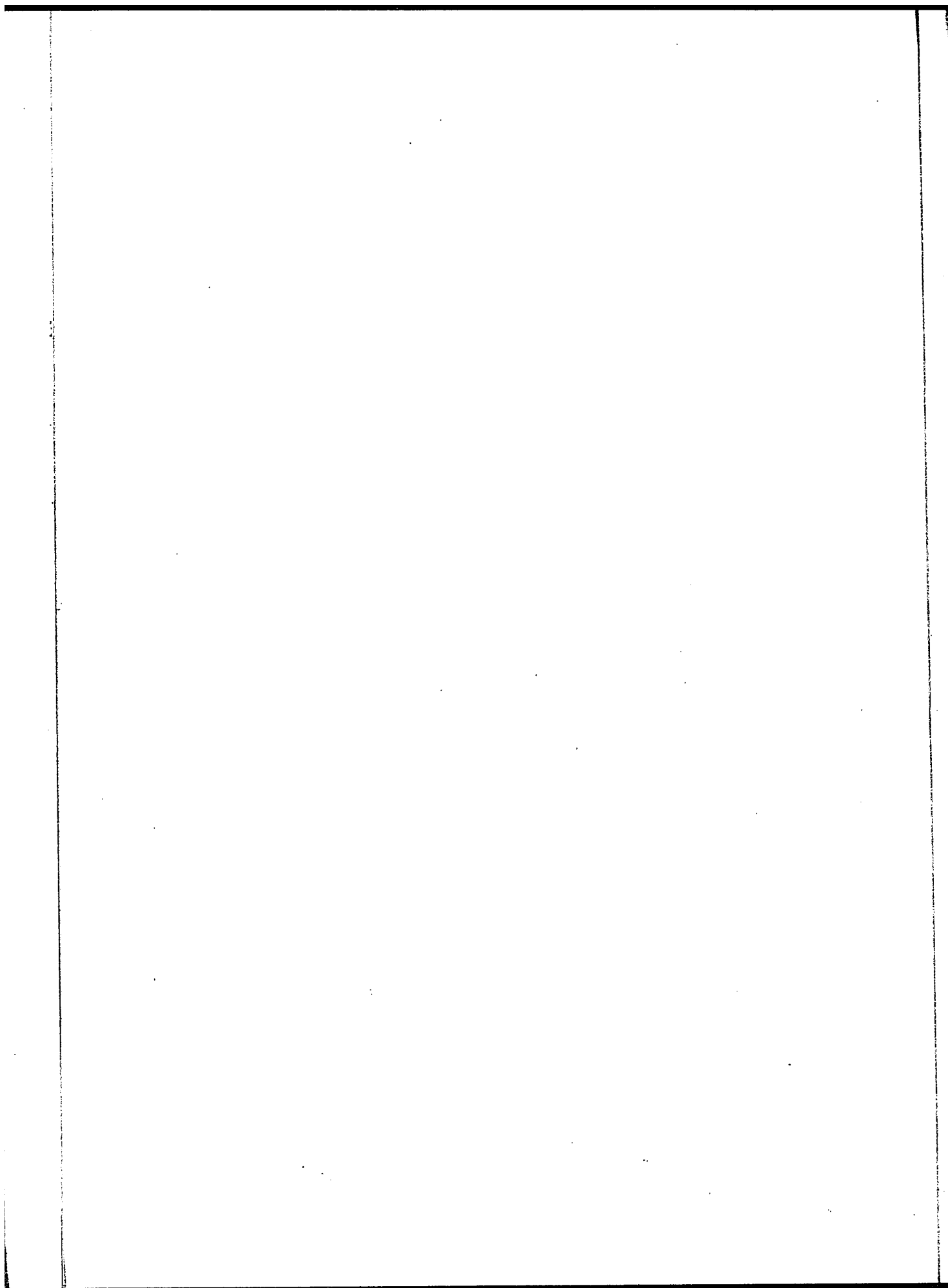
$$L_3 = 6 \mu H$$

$$T_1 = 6AG7$$

$$T_2 = 12AU7$$

$$T_3 = 6SA7$$

C_1^* C_2^* AND C_3^* ARE ZERO TEMPERATURE COEFF. MIKA CONDENSERS



- (1) Variation in supply voltages;
- (2) Mechanical instability of the system;
- (3) Temperature variations;
- (4) Low Q coil;
- (5) Spontaneous variation of the oscillator tube parameters.

Description of the complete system.

The individual circuits are shown in figures 11 to 14. The fixed frequency oscillator used is a crystal controlled one with frequency shift less than 5 parts in 10^6 . The crystal is in an oven as recommended by the manufacturer.

The mixer is again a conventional one. The main source of possible frequency shift is the noise controlled oscillator. To make it as good as possible, the following things were done:

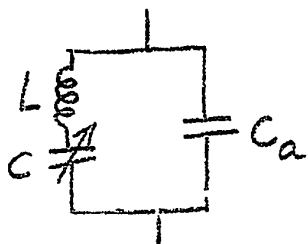
(1) To minimize the variations in the supply voltages, an additional voltage regulator was built in the oscillator chassis.

(2) To provide good mechanical stability the oscillator chassis was made of heavy 1/4" thick brass plate, and each component installed as strongly as possible.

(3) To minimize the effect of the temperature variation the oscillator was operated in an air conditioned room, and each capacitor which may have effect on the frequency was a zero temperature coefficient mica condenser.

(4) High "Q" coil was used. It was made of heavy copper wire wound on 2 1/2" diameter bakelite core, giving a Q of 400.

(5) To minimize the effect of the variation in the tube parameters the shown "series tuned parallel LC circuit" was used. The purpose of c_1 and c_2 is that being relatively large condensers parallel to the input of the tube, all the minute changes in the tube parameters will be absorbed by them with no appreciable effect on the frequency. To show the sensitivity of this circuit consider the following calculation:



The impedance of the circuit is

$$\frac{1}{Z} = \frac{1}{j\omega L + \frac{1}{j\omega C}} + j\omega C_a$$

$$\text{At } \omega = \omega_0, Z \rightarrow \infty \text{ and } \frac{1}{Z} = 0$$

Consequently

$$j\omega_0 C = j\omega_0 C_a (LC\omega_0^2 - 1)$$

and

$$\omega_0 = \sqrt{\left(1 + \frac{C}{C_a}\right) \frac{1}{LC}}$$

$$\omega_0 + \Delta\omega_0 = \sqrt{\left(1 + \frac{C + \Delta C}{C_a}\right) \frac{1}{L(C + \Delta C)}}$$

but $C \ll C_a$ and therefore after making the necessary simplifications, we get

$$\Delta\omega_0 = \frac{1}{2} \frac{\Delta C}{C} \omega$$

but $\frac{\Delta C}{C} = \frac{\Delta x}{x}$

Finally we get

$$\Delta x = \frac{2x}{f} \Delta f$$

Thus we see that the sensitivity of this circuit is the same as if C_a were not present. (See equation 6).

In our case the following values were used:

$$x = 4 \times 10^{-2} \text{ cm;}$$

$$C = 200 \mu\mu$$

$$C_1 = C_2 = 1000 \mu\mu$$

and $f = 4020 \text{ kc.}$

The crystal controlled oscillator was working at 1 Mc. Thus the difference frequency was obtained by beating the frequency of the noise controlled oscillator against the 4th harmonic of the crystal controlled one.

The sensitivity

$$\Delta x = \frac{2x}{f} \Delta f = \frac{8 \cdot 10^{-2}}{4 \cdot 10^6} = 2 \cdot 10^{-8} \text{ cm}$$

i.e. $\Delta f = 1$ corresponds to 2 \AA 's distance change. The noise controlled oscillator has a frequency shift of 50 c/15 minutes, but the short term stability was much better.

The time necessary to determine the noise between two successive positions of the stage was less than 30 seconds, so

that during this short time the frequency shift of the oscillator was negligible.

The time necessary to make a complete run of the noise measurement at a given cell length was less than 10 minutes. This is quite short in comparison with the interferometric method. Figure 15 shows the noise of the stage as a function of cell for the Koristka microscope (see reference 6) and for our stage. In the case of our stage, the noise is plotted as obtained by the interferometric method and by frequency measurement.

In conclusion we may say that it is possible to measure small distance variations more quickly and more accurately this way than by interferometry.

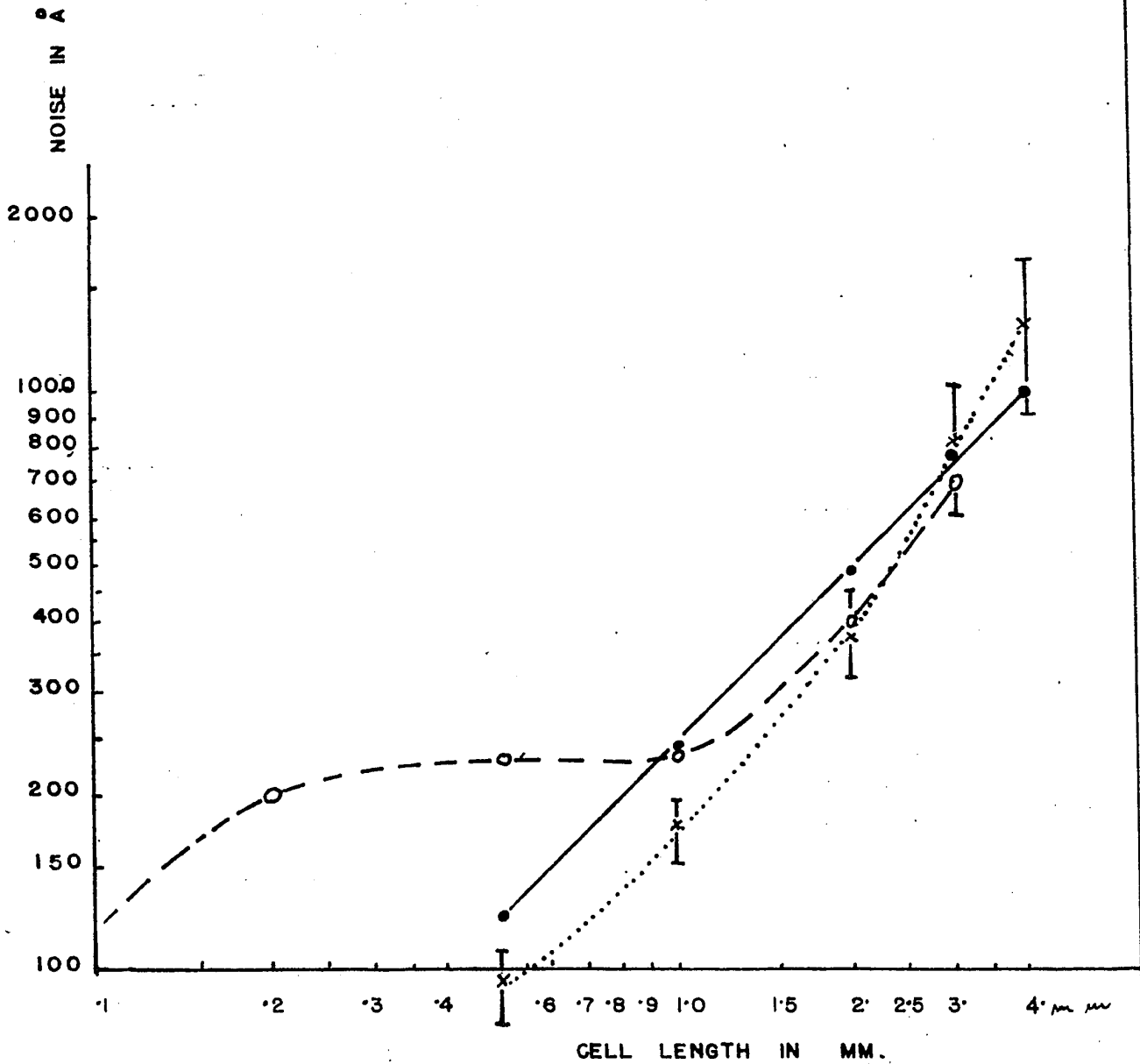


FIG. 15 STAGE NOISE VS CELL LENGTH.

BROKEN LINE: KORITSKA STAGE (MS - 2)

CONTINUOUS LINE: OUR STAGE (MEASURED INTERFEROMETRICALLY)

DOTTED LINE: OUR STAGE (OBTAINED BY FREQUENCY

MEASUREMENT)

PART II.

INTERACTION OF 6.2 BEV. PROTONS WITH THE EMULSION NUCLEI.

The interaction of high energy protons with individual nucleons has been the subject of numerous publications. The multiplicity and the angular distribution of the pions produced have been measured for various proton energies. Such measurements can also be made in the case of collisions of high energy protons with nuclei, but the interpretation of the results would require the knowledge of the number of target nucleons directly involved in the interaction and the processes involved in pion emission.

The application of the tunnel theory, see references (7), (8), (9), may help to give an interpretation of the experimental data obtained from the interaction of high energy protons with complex nuclei.

Purpose: To study the applicability of the tunnel theory to the interaction of 6.2 Bev. protons with the emulsion nuclei.

There are two main experimental results to be considered:

- 1) Multiplicity;
- 2) Angular distribution.

Multiplicity: First of all let us show that the total kinetic energy available for shower particle production in the C.M. system (center of mass system) at a given primary energy is an increasing function of the number of target nucleon masses. By target nucleon masses is meant the number of nucleons directly involved in the collision with the primary proton, and by C.M. system that system of coordinates in which the total momentum of the interacting particles is zero.

Notation: U^* : total energy in C.M. system.
 U_L : total energy in the laboratory system.
 β_c : relative velocity of the C.M. system.
 pc : momentum of the primary measured in energy units in laboratory system.
 M : rest mass energy of the nucleon.
 x : number of target nucleon masses.
 E_L : kinetic energy of the primary proton in the laboratory system.
 E^* : total kinetic energy available in the C.M. system.

$$(7) \quad U^* = U_L \sqrt{1 - \beta_c^2} = U_L \sqrt{1 - \frac{(P_c)^2}{U_L^2}} = \sqrt{U_L^2 - (P_c)^2}$$

$$= \left\{ [(E_L + \mu) + \mu x]^2 - (P_c)^2 \right\}^{1/2}$$

$$\text{but } (E_L + \mu)^2 - (P_c)^2 = E_L^2 + \mu^2 + 2\mu E_L - E_L^2 - 2\mu E_L = \mu^2$$

$$\text{Consequently } U^* = \sqrt{\mu^2 + 2\mu x (E_L + \mu) + \mu^2 x^2}$$

and

$$(8) \quad E^* = U^* - (x+1)\mu$$

which says exactly as stated above; namely, that the kinetic energy increases with increasing number of target nucleon masses x in the C.M. system at a given primary energy, see fig. 16.

After this introduction let us describe the tunnel model of the high energy interactions.

Tunnel theory: At high enough energies the incoming primary punches a hole called the tunnel through the target nucleus and the nucleons which before the interaction were within the tunnel will leave the nucleus as a sub-nuclear mass containing the primary and sharing its energy. The residual excited nucleus will then cool off by "evaporating" slow secondaries. If this is the case, then the emission of pions from the sub-nuclear mass having high excitation energy is quite independent from the evaporation process. The shower multiplicity would depend on the tunnel length, i.e. on the radius

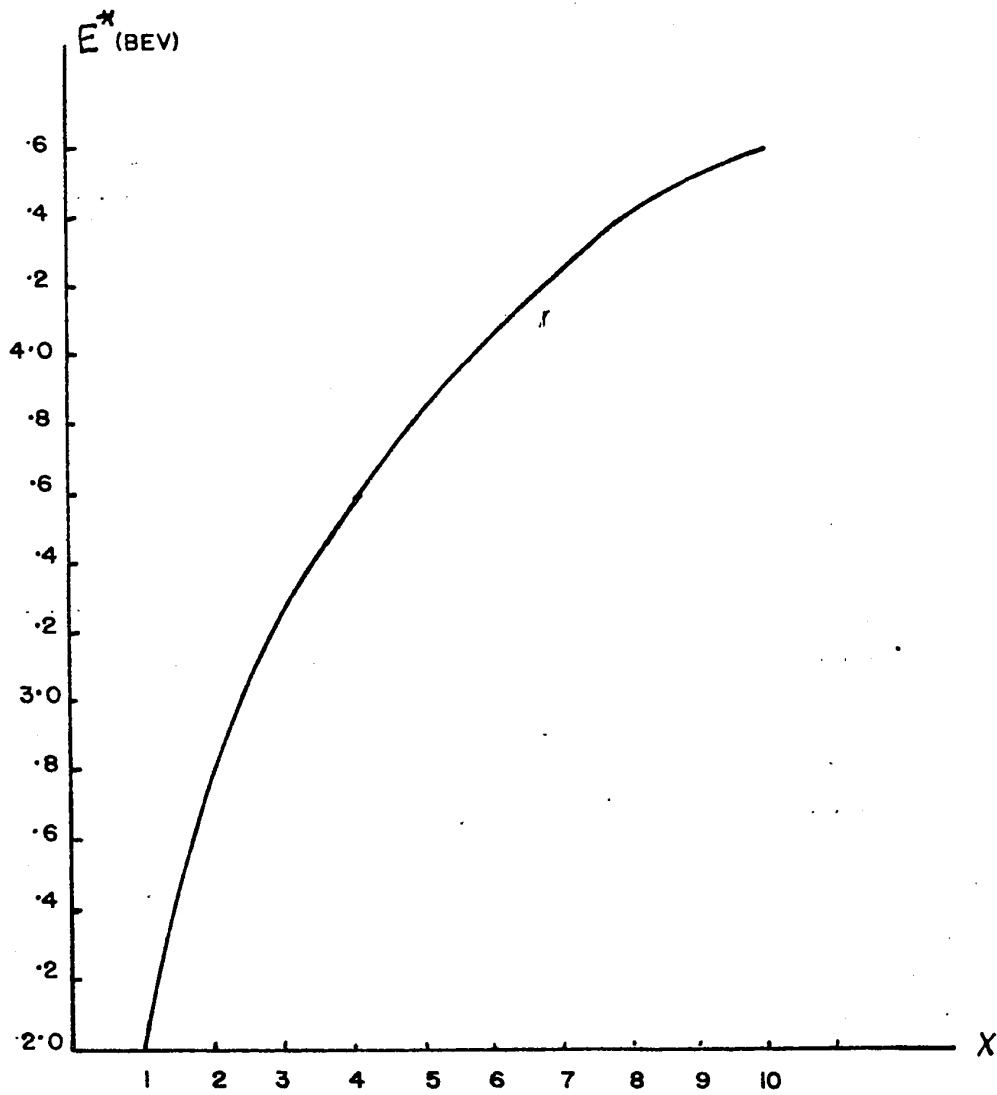


FIG 16 KINETIC ENERGY AVAILABLE IN C.M. SYSTEM AS A FUNCTION OF X THE NUMBER OF TARGET NUCLEON MASSES, AT A PRIMARY ENERGY OF 6.2 BEV.

of the target nucleus.

To apply this picture to the emulsion plates it should be mentioned first that the nuclei of the atoms forming the emulsion can be divided into two groups:

- 1) "L" - group containing the light elements,
namely H, C, N, O;
- 2) "H" - group which contains the heavy elements:
Br, Ag.

This means that the primary has a chance to interact with any of these nuclei. It is customary, however, to restrict the investigation to "H" or "L" - groups instead of specifying the exact atomic number of the nucleus which, in general, would be a very difficult experimental task. Therefore, in this work it will be assumed that the emulsion contains two kinds of target nuclei only: the "L" nuclei with mass number ≈ 14 and the "H" nuclei with mass number ≈ 95 .

Under these conditions the tunnel theory predicts two different multiplicities for the shower particles. This is obvious because the multiplicity is a function of the nuclear radius and there are two mean radii within the emulsion as explained above. Thus, plotting the shower multiplicity as a function of the number of heavy prongs (evaporation secondaries), it is expected to get a step-like shape.

Angular distribution: The problem in this case is to find the effective C.M. system of the interaction system using the distribution of the emitted pions in the laboratory system. To do this we need to know the transformation equation of the angles between the two systems of reference.

Transformation equation of angles: The simplest way to find the transformation equation is to start with the Lorentz transformation of velocities.

Let the system S' move with respect to S with a velocity u along the x axis and let the particle have a velocity v' in S' , its components being v'_x , v'_y , and $v'_z = 0$. Mathematically, this last condition ($v'_z = 0$) would mean a loss of generality. It is easy to see, however, that this condition means that the x, y plane is oriented in such a way as to make the z component of the velocity equal to zero. As long as we keep this in mind the expression to be derived will have a general meaning.

It is well known that under this condition the velocity v' can be described in S by the following relations:

$$(9) \quad v_x = \frac{v'_x + u}{1 + \frac{v'_x u}{c^2}} \quad , \quad v_y = \frac{v'_y}{1 + \frac{v'_x u}{c^2}} \sqrt{1 - \frac{u^2}{c^2}}$$

but

$$v_x = v \cos \theta \quad \text{and} \quad v'_x = v' \cos \theta'$$

$$v_y = v \sin \theta \quad \quad \quad v'_y = v' \sin \theta'$$

substituting these into (9) we get

$$(10) \quad v \cos \theta = \frac{v' \cos \theta' + u}{1 + \frac{v' \cos \theta' u}{c^2}}, \quad v \sin \theta = \frac{v' \sin \theta'}{1 + \frac{v' \cos \theta' u}{c^2}} \sqrt{1 - \frac{u^2}{c^2}}$$

the division of these equations gives

$$(11) \quad \operatorname{tg} \theta = \frac{v' \sin \theta'}{v' \cos \theta' + u} \sqrt{1 - \frac{u^2}{c^2}} = \frac{1}{\gamma_u} \frac{\sin \theta'}{\cos \theta' + u/v'}$$

Equation (11) gives the transformation equation of angles between the C.M. and the laboratory system if u is the velocity of the C.M. system with respect to the laboratory frame of reference, and v is the velocity of the particle in C.M.

Taking the logarithm of equation (11) we get

$$(12) \quad \log \operatorname{tg} \theta_L = -\log \gamma_u + \log \left(\frac{\sin \theta'}{\cos \theta' + \beta c/p'} \right)$$

It has been shown by Castagnoli, see reference (10), that plotting the number of pions emitted vs. $\log (\operatorname{tg} \theta_L)$, one gets a gaussian distribution about the average which is $\log \gamma_u$

whose standard deviation ζ contains the information about the symmetry properties in C.M. system. Namely, if $\zeta = .36$, the distribution of the pions in C.M. system is spherically symmetrical and if $\zeta > .36$, there is a forward - backward peaking. With increasing ζ the deviation from spherical symmetry increases. The deviation x from spherical symmetry, however, would still mean symmetry with respect to the x plane perpendicular to the direction of motion of the primary particle. This simply means that in C.M. system there are as many pions emitted forward as backward.

If the emitted pions are the result of the interaction of the primaries of mono-kinetic energy with one type of nuclei (i.e. L or H), then taking the average of both sides of equation (12) over all the pions emitted, the equation becomes

$$(13) \quad \frac{1}{n} \sum_{i=1}^n \log \operatorname{tg}(\theta_i) = -\log \gamma_c + \frac{1}{n} \sum_{i=1}^n \log \left(\frac{\sin \theta_i}{\cos \theta_i + \frac{\beta_c}{\beta_{\pi}}} \right)$$

Now, assuming that:

- 1) There is a single average kinetic energy for the emitted pions in C.M.
- 2) There is a symmetry for the number of pions emitted with respect to the plane perpendicular to the direction of motion of the primaries.

3) The velocity of the C.M. system with respect to the laboratory system is equal to the velocity of the pions in the C.M. system, i.e. $\beta_c = \beta_\pi$,

then it can be shown that

$$\frac{1}{n} \sum_{i=1}^n \log \left(\frac{\sin \theta'_i}{\cos \theta'_i + \beta_c / \beta_\pi} \right) = 0$$

consequently

$$(14) \quad \log \delta_c = - \frac{1}{n} \sum_{i=1}^n \log \operatorname{tg}(\theta'_i).$$

Thus it is possible to calculate the number of target nucleon masses x from the emission angles of pions as measured in the laboratory system.

We should be aware, however, that in obtaining x in this way we have made three assumptions. Let us see if they are justified.

1) It is an experimental fact, see reference (11), that most of the emitted pions have energy in C.M. system distributed about an average (in this energy range) of 250 Mev. On this basis, this assumption in the first approximation can be accepted.

2) The symmetry property is again an experimental fact (see eg. (12)), so that this assumption should be valid also.

3) This assumption should be checked with the value of x obtained. If we find that $\beta_c \neq \beta_\pi$ contrary to the assumption, then the next step should be to find out what error was introduced.

Fortunately it is possible to find the C.M. system without using assumption 3.

a) One way is to plot the distribution of pions in different C.M. systems and selecting that system in which there is the best symmetry. This plot can be done in the following way: Making use of equation (11).

$$\operatorname{tg} \theta_L = \frac{\sin \theta_{c.n.}}{\cos \theta_{c.n.} + \beta_c / \beta_\pi} \sqrt{1 - \beta_c^2}$$

and

$$\operatorname{tg} \theta_{c.n.} = \frac{\sin \theta_L}{\cos \theta_L - \beta_c / \beta_\pi} \sqrt{1 - \beta_c^2}$$

and assuming 250 Mev. for the kinetic energy of the pions in the C.M. system it is possible to trace the relation $\theta_{c.n.} = f(\theta_L)$ for different target masses, see figure 17. Using this curve, all the angles measured in the laboratory system can be transformed to the assumed C.M. system. We can then plot the differential distribution of pions vs. $\cos \theta_{c.n.}$

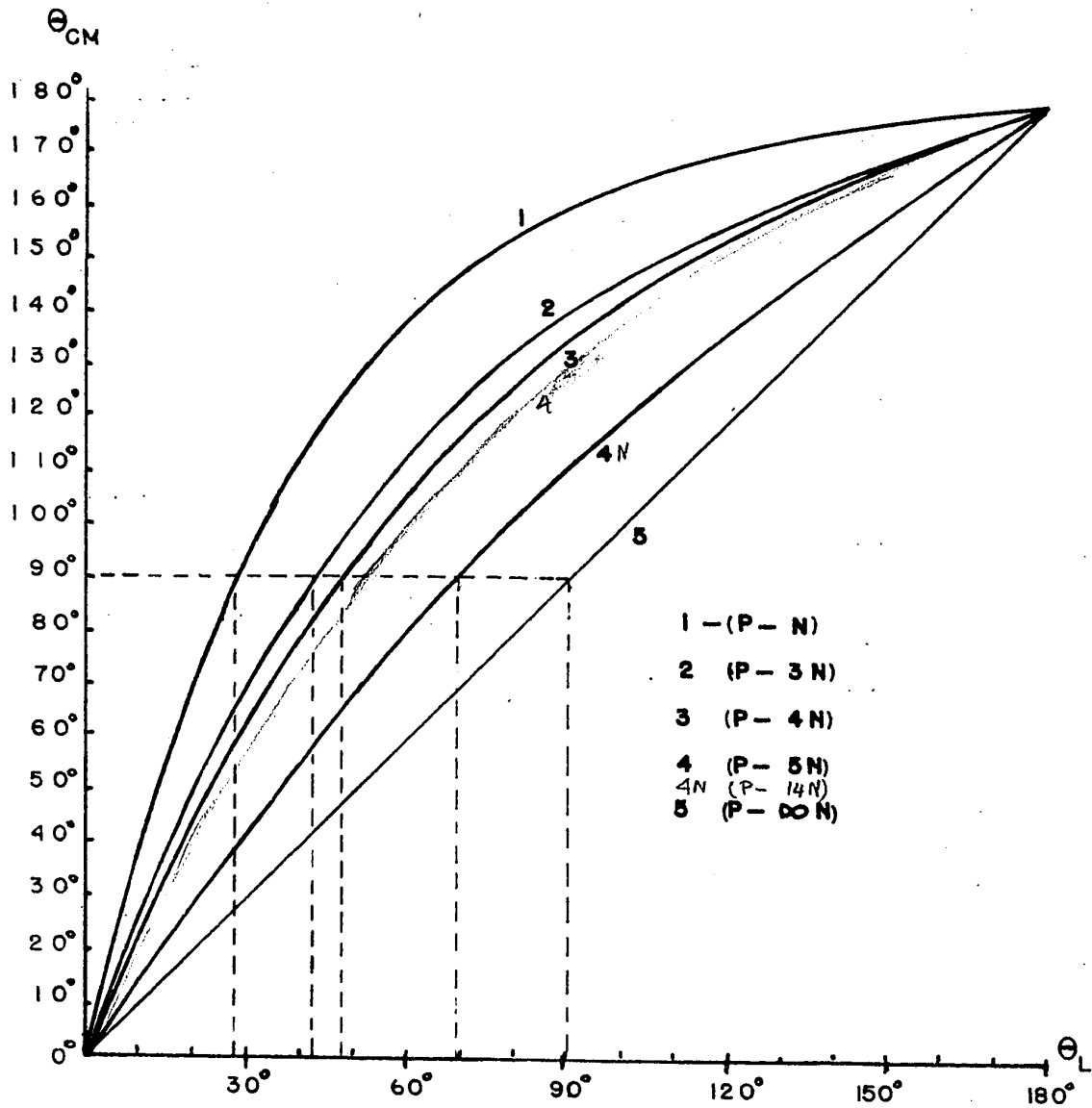


FIG. 17 CURVES REPRESENTING THE TRANSFORMATION OF ANGLES BETWEEN THE LAB. SYSTEM AND DIFFERENT C.M. SYSTEMS.

b) The other way is to determine the half angle; the half angle is by definition that angle as measured in the laboratory system within which half of the pions are emitted. This angle of course would correspond to 90° in the C.M. system. To see how the half angle is connected to the number of target nucleon masses consider the transformation equation of angles:

$$\operatorname{tg} \theta_L = \frac{\sin \theta_{ch}}{\cos \theta_{ch} + \beta_c / \beta_\pi} \frac{1}{\gamma_c}$$

Let $\theta_{ch} = 90^\circ$ and $\theta_L = \theta_{1/2}$ then the transformation equation becomes:

$$(15) \quad \operatorname{tg} \theta_{1/2} = \frac{\beta_\pi}{\beta_c} \frac{1}{\gamma_c} = \beta_\pi \sqrt{\frac{1}{\beta_c^2} - 1}$$

but

$$\beta_c = \frac{(P_c)}{U_L}$$

substituting this into (15), we get

$$(16) \quad \operatorname{tg} \theta_{1/2} = \beta_\pi \sqrt{\frac{U_L^2}{(P_c)^2} - 1} \quad \text{where } U_L = E_p + (x+1)\mu$$

Writing U_L in its explicit form, then from equation (16) we finally get:

$$(17) \quad x = \frac{1}{\mu} \left\{ (P_c) \sqrt{1 + \frac{\operatorname{tg}^2 \theta_{1/2}}{\beta_\pi^2}} - E_p \right\} - 1$$

So that by measuring the kinetic energy of the primary and the half angle we can calculate x , the number of target nucleon masses.

Let us now discuss the physical significance of the number of target nucleons as calculated above. As defined previously the C.M. system is that system of coordinates in which the total momentum of the interacting particles is zero. Consider, for example, the interaction of the high energy protons with the heavy nuclei. Assuming the tunnel theory to be valid for the interaction, then most of the primary energy is distributed over the volume containing the sub-nuclear mass which has been pushed out of the tunnel. This means that the interaction takes place between the primary and the sub-nuclear mass as a unit. Consequently the C.M. system consists of the primary particle and another "particle" whose mass is equal to the volume occupied by this "particle", (volume of the tunnel), multiplied by the density of nuclear matter.

EXPERIMENTAL PART

Procedure: The plates used were part of a large stack of Ilford G-5 emulsion exposed to the 6.2 Bev. proton beam from the Berkeley bevatron. Approximately 4.8 cm³ emulsion having the dimensions of 10 cm x 15 cm x 600 μ has been area scanned with a magnification of 120X. This way the large stars have been detected and most of the small ones missed. All the shower tracks of sufficient length have been graincounted and their energy determined by multiple scattering with the accuracy necessary to identify the shower particles. If the track was too short to give a sufficiently accurate determination of momentum and thus to identify the particle, then the track was considered as steep. An appreciable number of steep tracks were found in this way and the number of pions amongst ^{them} was determined from the ratio of pions to protons obtained from the set of identified particles. From the data the shower multiplicity has been calculated and compared with the theoretical prediction. The angular distribution of pions has been plotted using the identified pions only. Finally, the pion multiplicity was calculated, using all the shower particles.

Shower multiplicities: The experimental results are shown in tables 1, 2, and 3. In table 1, the 2nd and 3rd columns show the number of events described in the 1st column for "H" and "L" target nuclei, respectively. For instance, we see that the total number of stars is 78, where 55 of these belong to "H" group and 23 to "L" group. We have a total of 1115 tracks in these 78 stars, 924 of them belong to the "H" stars and 191 to the "L" stars. We have counted as light tracks all those with a grain count $\leq 2.5 g^*$, where g^* is the normalized grain density. All other tracks are considered as heavy (N_h). The light tracks are called the shower tracks (n_s), and we shall deal with them later.

	H	L	total
No. of stars	55	23	78
Total No. of tracks	924	191	1115
No. of heavy prongs	593	81	674
No. of light tracks	331	110	441

TABLE I.

	H	L	total
No. of pions	64	33	97
No. of protons	148	48	196
No. of steep tracks	119	29	148

TABLE 2.

Table 2 shows the number of pions, protons and steep tracks among the 441 shower particles.

Finally, table 3 shows in detail the data included in table 1. The purpose of this table is to calculate the shower multiplicities in different ranges of N_h . Column 1 shows the frequencies of stars having N_h heavy tracks as indicated in column 2, and the number of shower particles n_g as indicated in column 3. Column 4 shows the average multiplicity, i.e. the number of shower particles per star in the intervals shown.

TABLE III

No. of stars	N_h	n_g	Multiplicity
3	0	7, 4, 7	$\frac{87}{17} = 5.1 \pm .5$
	1		
3	2	8, 5, 5 (1 k-particle)	
	3		$\frac{98}{19} = 5.2 \pm .5$
11	4	4, 5, 4, 3, 4, 6, 3 6, 6, 7, 3	
8	5	2, 3, 8, 6, 8, 6, 4, 2	
4	6	6, 7, 4, 4	$\frac{114}{18} = 6.3 \pm .5$
7	7	5, 5, 4, 8, 4, 9, 3	
4	8	5, 6, 6, 3	
9	9	7, 9, 6, 9, 5 4, 3, 6, 2	$\frac{125}{19} = 6.5 \pm .5$
5	10	5, 6, 11, 5, 4	
3	11	6, 7, 8	
3	12	6, 6, 4	$\frac{125}{19} = 6.5 \pm .5$
6	13	7, 9, 8, 8, 6, 11	
2	14	5, 4	
2	15	9, 9	
3	16	10, 4, 6	
1	17	4	
2	18	6, 7	
1	19	5	
1	23	2	

The shower multiplicities as given in column 4 of Table 3 are plotted in figure 18. It is interesting to observe the step-like shape as one would expect from the tunnel theory.

PION MULTIPLICITY

To calculate the correct multiplicity, we should consider the "L" and "H" groups separately. In doing this, however, we would introduce a large statistical error into the calculations on account of the relatively few light stars studied. Other experiments (reference 13) indicated that at a given primary energy the pion multiplicity for the "L" and "H" groups does not differ appreciably. Therefore, we shall not introduce a large error if we assume that the multiplicities are equal for the two groups, and calculate the overall pion multiplicity.

Figure 19 shows the energy distribution of all the shower particles with $p\beta \geq 1\text{Bev}$, and all those of lower energy for which a more accurate energy determination was necessary to identify them. An important observation is that the particles with energy higher than 1Bev are all contained within a 40° cone with respect to the direction of the primary, and only relatively few lie within a 10° cone. On the other hand, assuming 250 Mev kinetic energy for the pions in the C.M. system, it can be shown that it is highly

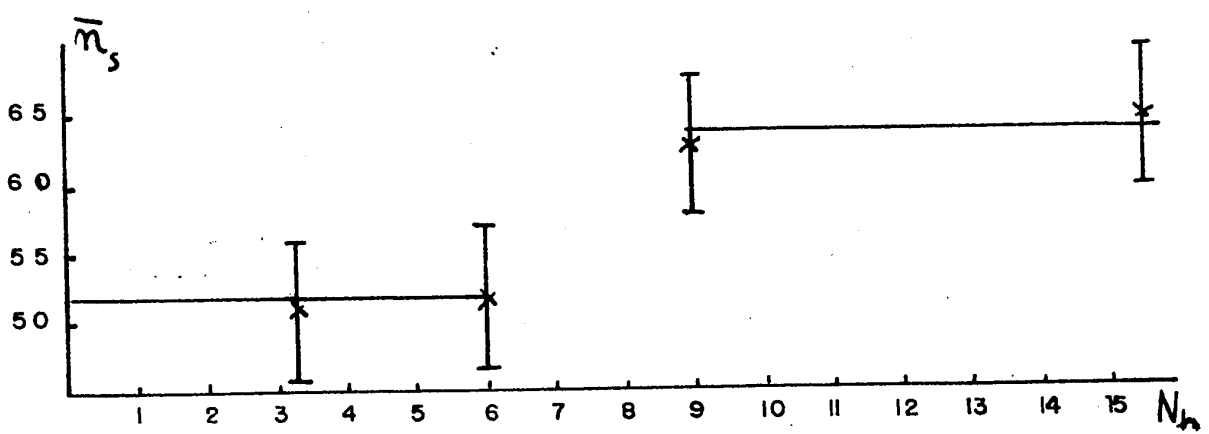


FIG 18 GRAPH SHOWING THE DEPENDENCE OF THE SHOWER MULTIPLICITY n_s ON THE NUMBER OF EVAPORATION SECONDARIES N_h

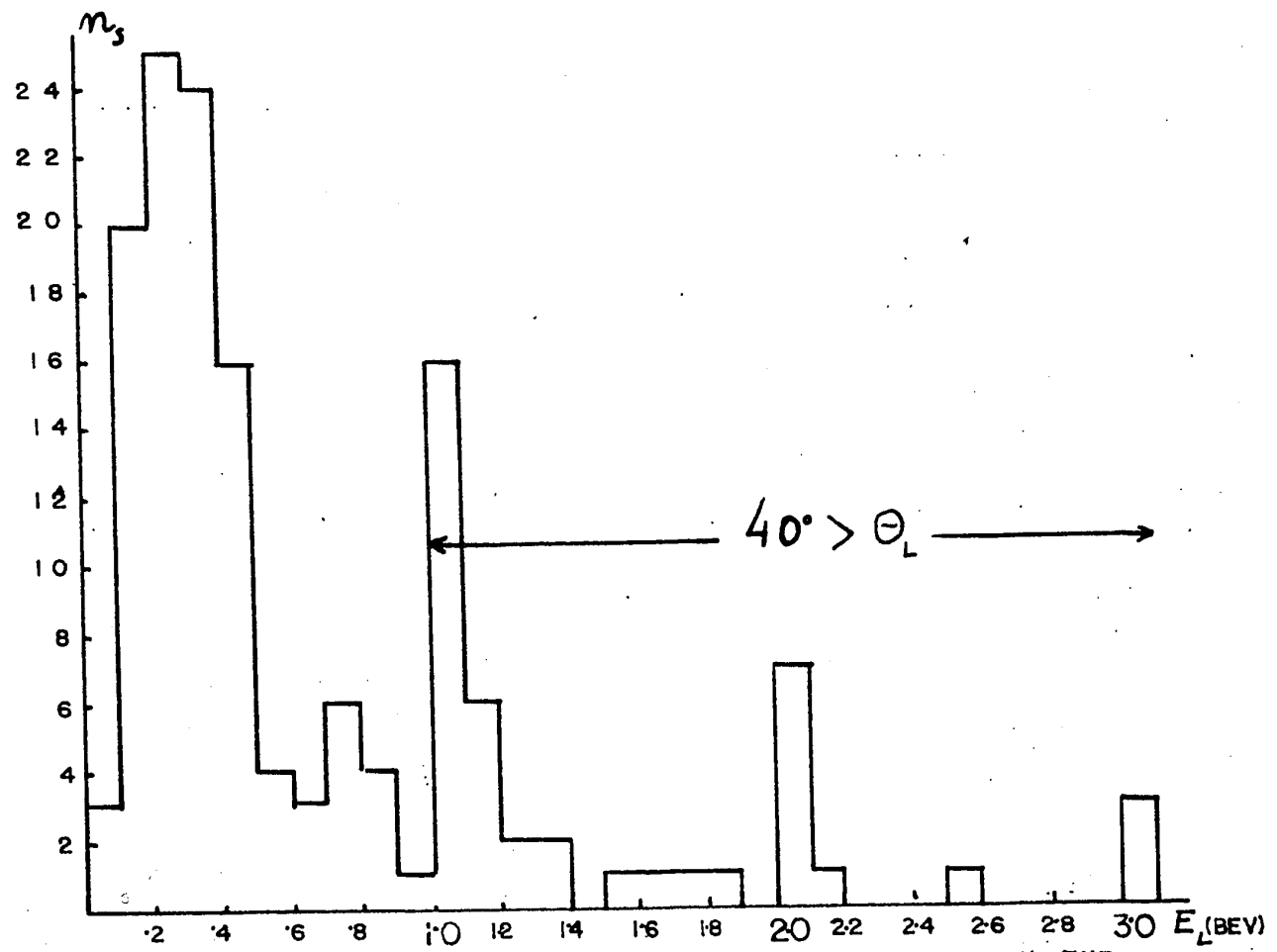


FIG 19 ENERGY DISTRIBUTION OF THE SHOWER PARTICLES IN THE LAB SYSTEM

improbable to find pions outside a 10° cone with energy higher than 1 Bev. Consequently it will be very unlikely to find pions amongst the $\mu\mu$ shower particles having energy greater than 1 Bev., and therefore it can be assumed that these particles found are all protons.

Returning to the steep tracks, it seems reasonable to assume that there are no secondaries included with energy greater than 1 Bev., simply because the angles are too large.

Now let us estimate the ratio of pions to protons among the steep tracks. The ratio of pions to protons for the set of steep tracks should be the same as the ratio for the identified set of particles, excluding the $\mu\mu$ particles which have too high an energy. So,

$$\frac{97}{196 - 44} = .638 = \frac{x}{148}$$

$$x = 94$$

where 148 is the total number of steep tracks. (see table 2).

This means that there should be 94 pions included in the 148 steep tracks. The multiplicity for the charged component of the emitted pions then is

$$n_{\pi^{\pm}} = \frac{191}{78} = 2.45 \pm .2$$

Assuming that 1/3 of the total number of pions produced are neutral, we get for the total multiplicity

$$n_p^{0\pm} = 3.7$$

In order to calculate the tunnel dimensions, expressed in proton masses, it will be helpful to discuss the physical meaning of the shower particles.

On reading the literature, one discovers that several different criteria are applied to the selection of the shower particles. Some authors consider secondaries to be shower particles if their grain density is higher than 1.4 times minimum, whereas others use a value of 1.6. Under these circumstances, it is not difficult to arrive at the conclusion that there is no clear-cut definition of shower particles.

We shall attempt to give a physical definition of the shower particles by defining an effective impact parameter for the interaction of the primary with the emulsion nuclei.

Let us define our maximum impact parameter such that, in the case of interaction, the energy available in the C.M. system is just sufficient for pion production. (This energy will be of the order of 150 Mev.). This definition means that the shower particles are those secondaries which have been involved in a direct collision with the primary particle

within the nucleus at an impact parameter less or equal to that calculated from the energy considerations. Moreover, all the pions produced will be shower particles, irrespectively of their energy, since they result from a collision between the primary and a nucleon for which the impact parameter is less than the calculated maximum.

The maximum impact parameter may be calculated using the following relativistic equations:

$$\begin{aligned} U^* &= U_L \sqrt{1 - \beta_c^2} \\ U^* &= E^* + (1 + x')\mu \\ U_L &= E_p + (1 + x')\mu \end{aligned}$$

On simplifications we get

$$x' = \frac{E_p^2 - (P_c)^2 - E^{*2}}{2\mu(E^* - E_p)}$$

which gives for $E^* = 150$ Mev. at a primary energy of 6.2 Bev. a value of $x' = .02$ protons mass. If we assume a uniform structure or density for the proton, thus an edge on collision should be sufficient to produce a meson.

After this preliminary discussion, let us calculate the tunnel dimensions.

$$\begin{aligned}
 R_H &= R_0 A_H^{1/3} \\
 &= R_0 (95)^{1/3} \\
 &= 4.6 R_0
 \end{aligned}$$

where R_H is the radius of the heavy nuclei, R_0 is the proton radius, and A_H is the atomic mass of the "H" nuclei.

The volume of the tunnel will be equal to the cross sectional area of the primary proton multiplied by the effective tunnel length, which is two thirds of the diameter of the nucleus, i.e.:

$$\begin{aligned}
 V_t &= [(2 \cdot 4.6 R_0)^{2/3}] \pi R_0^2 \\
 &= 4.6 \times \frac{4}{3} \pi R_0^3 \\
 &= 4.6 \times V_p
 \end{aligned}$$

where V_t and V_p are the volumes of the tunnel and a proton respectively.

The obtained value means that the primary proton will collide with 4.6 nuclear masses.

Assuming that 50 percent of these are neutrons, and thus not registered among the shower particles, there should be 2.3 protons on the average, among the shower particles.

So far we have not included the primary escaping from the nucleus. Assuming a 50 percent charge exchange, we find that the proton contribution to the shower multiplicities, for the "H" nuclei

$$n_H = 2.8$$

and doing this calculation for the "L" stars also, we get

$$m_L = 1.7$$

Including the charged pion multiplicities we should find the following shower multiplicities for the "H" and "L" groups of target nuclei:

$$(m_s)_H = 5.3$$

and

$$(m_s)_L = 4.2$$

These are lower values than the experimental ones, but they are systematically lower for the "H" and "L" groups. This means that the criterium for the selection of shower protons, i.e. all those with $g \lesssim 2.5 g^*$, is too large; a value of $g \lesssim 2.0 g^*$ would give a much better agreement between the theory and experiment.

Angular Distribution: The plotting of the angular distribution should be done for the two different target nuclei separately but due to the relatively few pions found we can plot the overall distribution and this way find the masses involved in the pion producing collision.

The finding of these masses will be done in three different ways:

1) From the determination of the half angle: Figure 2³ shows the angular distribution of 74 pions in the laboratory system. The angles have been determined with an error of less than 30°.

The half angle was found to be 42° 30'. Using this angle and 250 Mev. for the kinetic energy of the emitted pions, then from equation

$$\beta_{\pi}^2 = \frac{(P_c)^2}{\mu_c^2} = .87$$

and

$$\begin{aligned} \kappa &= \frac{1}{.937} \left\{ 7.07 \sqrt{1 + \frac{.83}{.87}} - 6.2 \right\} - 1 \\ &= 2.9 \end{aligned}$$

This calculation indicates three target nucleon masses participating in the pion producing collision.

2) From the determination of γ_c : As a first step let us see what kind of symmetry is there in G.M. system for the pions

emitted? Is it spherical or rather conical? The answer to this question will be given by σ the standard deviation of the gaussian distribution.

Figure 20 shows the differential distribution vs. $\log(\text{tg}\theta_L)$ for the 74 pions whose distribution is in the laboratory system shown in figure 27. The histogram shows the experimentally found distribution and the continuous curve the best fit gaussian curve. For tracing the curve it is necessary to know two parameters namely the average $\bar{x} = \frac{1}{n} \sum x_i$ and the standard deviation σ which is the second moment about the average \bar{x} . The results obtained are:

$$\bar{x} = .138 \quad \text{and} \quad \sigma = .39$$

which indicates that the distribution is nearly spherically symmetrical.

To see whether the gaussian distribution is the best fit statistical law describing the distribution of pions, let us apply the χ^2 -test. (See Appendix)

Using equation 18 we obtain $\chi^2 = 12.3$ and for the degrees of freedom $F=14$. Using these values, from figure 28 we get $P = .6$. This means that 4 out of 10 repetition of the same experiment we would not get higher statistical deviation from the assumed gaussian distribution. Therefore we see that even these relatively few pions used for tracing the

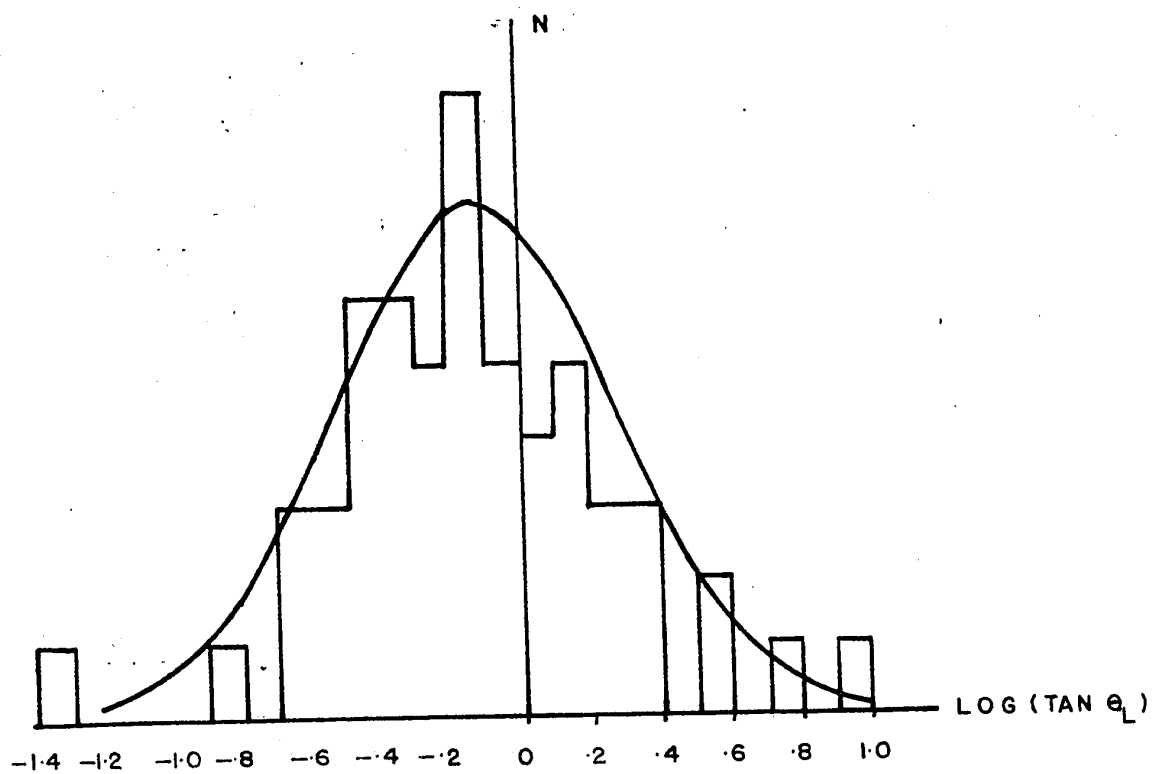


FIG. 20 THE HISTOGRAM SHOWS THE EXPERIMENTALLY OBTAINED DIFFERENTIAL DISTRIBUTION, AND THE CONTINUOUS CURVE THE BEST FIT GAUSSIAN CURVE.

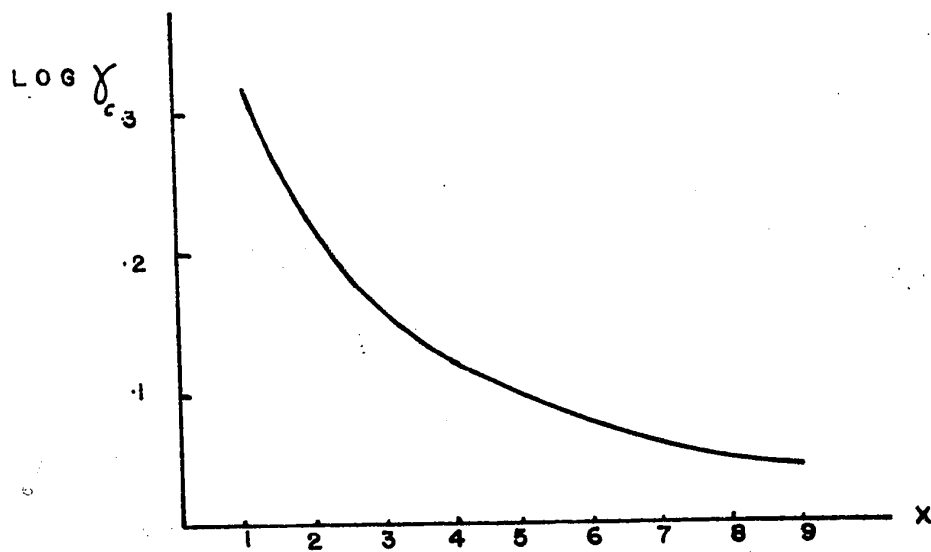


FIG. 21 CURVE SHOWING THE DEPENDENCE OF $\text{LOG } \gamma_c$ ON THE NUMBER OF EFFECTIVE NUCLEON MASSES

distribution, give a sufficiently good statistical fit and the assumed gaussian distribution describes well the experimentally found one.

Having found $\bar{x} = \log \gamma_c$ we need to calculate the number of target nucleon masses. To do this, consider equation

$$u^* = \frac{u_L}{\gamma_c}, \quad \gamma_c = \frac{u_L}{\sqrt{\mu^2 + 2\mu x(E_L + \mu) + x^2 \mu^2}}$$

Tracing $\log \gamma_c$ vs. x , we obtain x for the known value of $\log \gamma_c$. This function is shown in figure 21. For $\log \gamma_c = .138$ we get $x = 3.3$, in good agreement with that obtained from the half angle.

3) From the distribution plotted in different C.M. systems: The graphs showing the distribution in different C.M. systems are shown in figure 22 and 26. The assumed target nucleon masses are 1, 2, 3, 4, and 5 respectively. The dotted line through the middle of the graphs indicate the plane perpendicular to the direction of motion of the primary, and the numbers indicate the number of particles emitted forward and backward with respect to that plane.

The distribution representing 1, 2, 5 and higher target nucleon masses do not give symmetrical distribution, and

therefore it is very probable that the pion producing collision of the primary did not happen with these number of nucleons.

Considering the standard deviation for N events as $\pm \sqrt{N}$ we can only say that 3 or 4 target nucleon masses were responsible for the production of pions.

Let us compare this value to the value expected from the tunnel theory:

We have calculated the effective target nucleon masses to be 4.6 and 2.4 proton masses for the "H" and "L" target nuclei respectively. The angular distribution is an overall distribution for the two target nuclei, and therefore we have to calculate the overall effective target nucleon masses:

$$\frac{4.6 \times 55 + 2.4 \times 23}{78} = \frac{308.2}{78} = 3.9$$

which is in very good agreement with the experimental values.

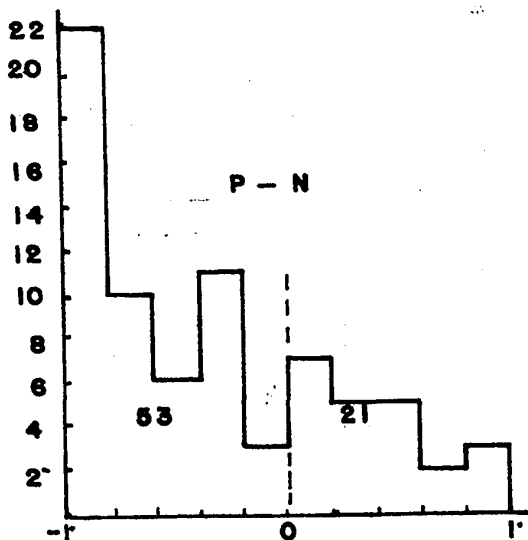


FIG 22

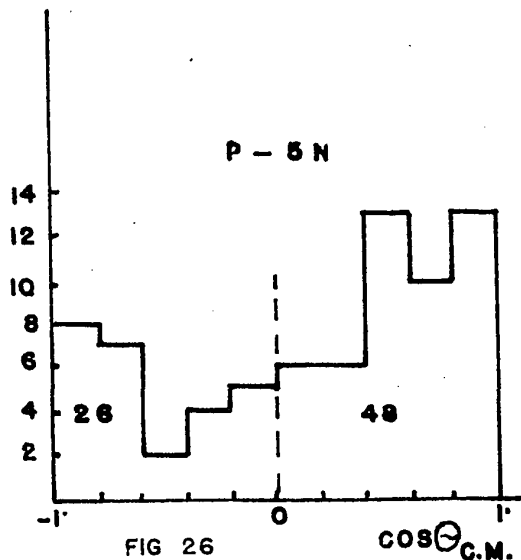


FIG 26

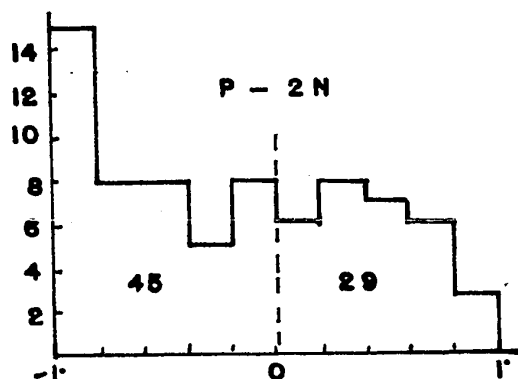


FIG 23

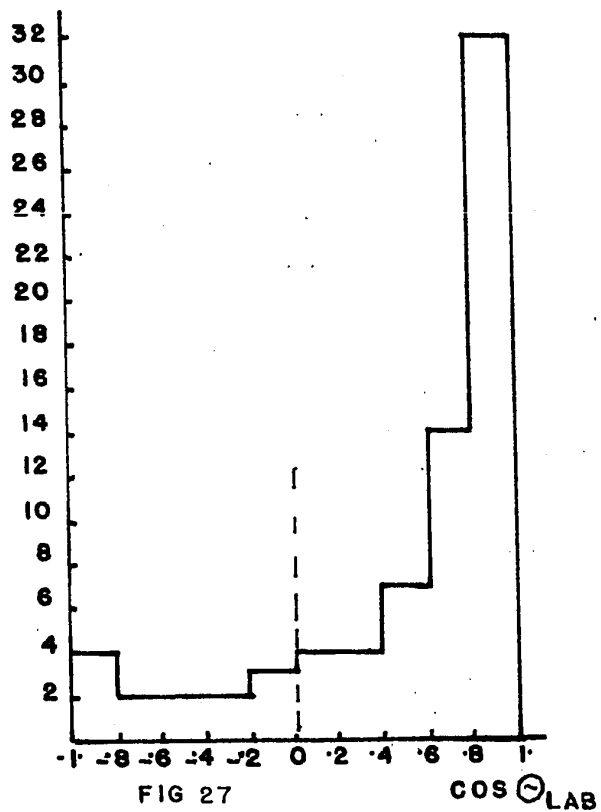


FIG 27

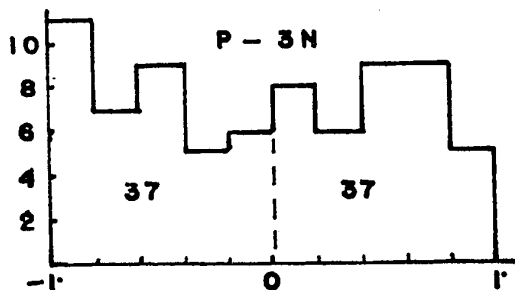


FIG 24

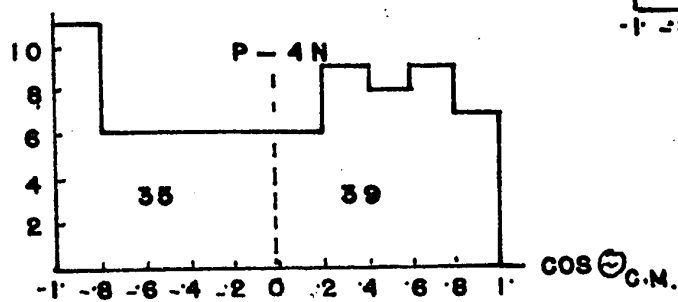


FIG 25

DISTRIBUTION OF
PIONS IN DIFFERENT
C.M.- SYSTEMS.

CONCLUSION

From the analysis of the stars the following results were obtained: Two different shower multiplicities are found for the "L" and "H" - groups of target nuclei; The mean number of shower particles are:

$$(n_s)_H = 6.4 \pm .4$$

and

$$(n_s)_L = 5.1 \pm .5$$

The mean number of charged and the probable total pion multiplicities are:

$$n_{\pi}^{\pm} = 2.5 \pm .2$$

and

$$n_{\pi}^{0\pm} = 3.7$$

From the angular distribution of pions in the laboratory system we have found the expected symmetrical distribution in the C.M. system, using 3 or 4 target nuclear masses. This means that only a small fraction of the nucleus takes part in the pion producing interaction of the primary.

The number of pions found of 3.7 (per star) is in agreement with the kinetic energy available in C.M. system consisting of the incoming primary and 3 or 4 target nucleons. The coefficient of inelasticity in this system is approximately 33 percent, whereas it would have to be about 70 percent if

we had assumed a proton-nucleon collision, in contradiction with the well established value of 33 percent.

We must stress the importance of the definition of the shower particles. The term "shower" particle originated from the very high energy interactions for which the convention of a grain density $\leq 1.4 \times$ minimum is logical. However, applying this criterion in the case of much lower energy interactions without even reconsidering its definition is not only illogical, but may lead to basically wrong conclusions. Good illustrations of this can be found in many of the recent publications (see for instance 14,) in which the authors arrive at the conclusion that in the collision of a proton with a heavy nucleus, the proton interacts with only one nucleon, or even a fraction of a nucleon in the whole complex nucleus.

All the results we have obtained (even the reconsideration of the definition of shower particles) are in agreement with the tunnel theory. Consequently, as far as these experimental results are concerned, we may conclude that the tunnel theory of nuclear interactions seems to be valid.

It would be interesting to compare these experimental results with the predictions of the theory of nuclear cascades. Unfortunately no data for an energy of 6.2 Bev. has been published as yet.

APPENDIX.

Sometimes it is necessary to answer the following questions: what kind of statistics describes an experimentally obtained distribution? What is the probability of getting higher statistical deviation from the observed one, if repeating the same measurement series? What is the reliability of the obtained statistical results? etc. These are the questions for which answer may be given using the Pearson's χ^2 test.

The technique of application of this test is quite simple.

It can be performed in three steps:

1) Obtain

$$(18) \quad \chi^2 = \sum_{i=1}^M \frac{((\text{observed value})_i^2 - (\text{expected value})_i^2)}{(\text{expected value})_i}$$

2) Determine the degrees of freedom F, i.e. the number of independent frequency intervals in which there is difference between the expected and observed values.

3) From the graph of Figure 28 get the probability P. This number shows the probability of having higher statistical deviation from the observed one if repeating the same experiment.

If $.1 \leq P \leq .9$, then the assumed statistics fits the experimental values obtained, if it is lower than .02 or

higher than .98 then the reliability of the experimental results is very questionable, or it may be that the chosen statistical distribution for calculating the expected values is not the correct one.

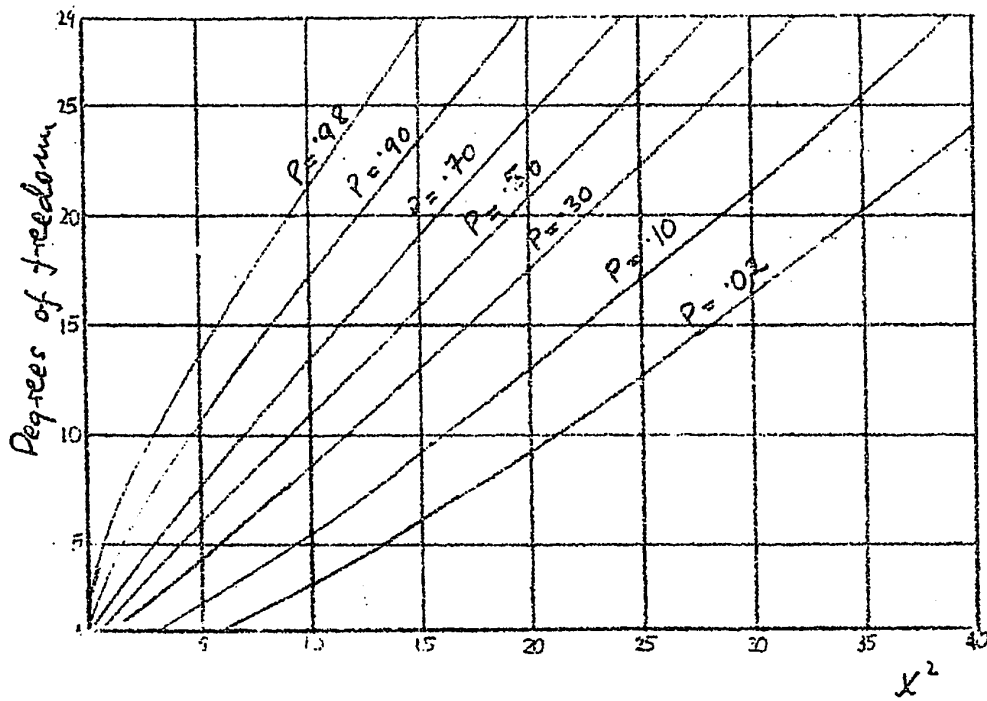


Fig. 28

 χ^2 - test

BIBLIOGRAPHY

- (1) B. Rossi: High Energy particles.
- (2) L. Voyvedic and E. Pickup: Phys. Rev. 85, 91 (1952).
- (3) L. Voyvedic: Progress in Cosmic Ray Physics, vol. II, chapter 5
- (4) J. Plainevaux: Nuovo Cimento 10, 1451 (1953).
11, 626 (1954)
12, 37 (1954).
- (5) Maddington: Proc. Roy. Soc. (1926).
- (6) Wissenberger: Exp. Tech. U.S.S.R. (1957).
- (7) F. Roesler and G. McCusker: Nuovo Cimento 10, 127 (1953).
- (8) G. McCusker and F. Koesler: Nuovo Cimento 11, 98 (1954).
- (9) W. Heitler and G. Terreaux: Proc. Phys. Soc. 66, 929 (1953).
- (10) G. Castagnoli et. al.: Nuovo Cimento 10, 1939 (1953).
- (11) K. Kalbach et. al.: Phys. Rev. 113, 330 (1959).
- (12) Lord Fainberg and Schein: Phys. Rev. 80, 970 (1950).
- (13) N. Metropolis et. al.: Phys. Rev. 110, 204 (1958).
- (14) V. Rajopadhye: Phil. Mag. 5, 537 (1960).

VITA

NAME: John Ancsin.
BORN: Békéscsaba, Hungary, 1933.
EDUCATED: Eötvös Lorand University Budapest - 1952-56.
University of Ottawa, 1957-60.
COURSE: Physics.
DEGREE: B.Sc. (honours) 1959.